ARGONNE NATIONAL LABORATORY
9700 South Cass Avenue
Argonne, Illinois 60439

THE URANIUM DISPERSION AND
DOSIMETRY (UDAD) CODE

Version IX,
A Comprehensive Computer Program to Provide Estimates of Potential
Radiation Exposure to Individuals and to the General Population
in the Vicinity of a Uranium Processing Facility

by

Michael H. Momeni, Yuchien Yuan,
and A. J. Zielen

Division of Environmental Impact Studies

Program Manager,
U. S. Nuclear Regulatory Commission:
Harold Peterson

May 1979

Prepared with the assistance of Timothy J. Biessel

and with acknowledgement to

Walter E. Kisieleski and

Carlyle J. Roberts

ABSTRACT

The Uranium Dispersion and Dosimetry (UDAD) Code provides estimates of potential radiation exposure to individuals and to the general population in the vicinity of a uranium processing facility. The UDAD Code incorporates the radiation dose from the airborne release of radioactive materials from uranium milling and processing facilities. It includes dosimetry of inhalation, ingestion and external exposures.

The removal of radioactive particles from a contaminated area such as uranium tailings by wind action is estimated from theoretical and empirical wind-erosion equations according to the wind speed, particle size distribution, and surface roughness and other parameters. Atmospheric concentrations of radioactivity from specific sources are calculated by means of a dispersion-deposition-resuspension model. Source depletion as a result of deposition, fallout of the heavier particulates, and radioactive decay and ingrowth of radon daughters are included in a sector-averaged Gaussian plume dispersion model. The average air concentration at any given receptor location is assumed to be constant during each annual release period, but to increase from year to year because of resuspension. Surface contamination is estimated by including buildup from deposition, ingrowth of radioactive daughters, and removal by radioactive decay, weathering and other environmental processes. Deposition velocity is estimated on the basis of particle size, density, and physical and chemical environmental conditions which influence the behavior of the smaller particles.

Calculation of the inhalation dose and dose rate to an individual is based on the ICRP Task Group Lung Model (TGLM). Estimates of the dose to the bronchial epithelium of the lung from inhalation of radon and its short-lived daughters are calculated based on a dose conversion factor from the BEIR report. External radiation exposure includes radiation from airborne radionuclides and exposure to radiation from contaminated ground. Terrestrial food pathways include vegetation, meat, milk, poultry, and eggs. Internal dosimetry is based on ICRP recommendations, with the option of using either a single or a multiple exponential retention model. In addition, individual dose commitments, population dose commitments and environmental dose commitments are computed.

Even though this code is dedicated to uranium mining and milling, it may be applied to dispersion of any other pollutant.

ACKNOWLEDGEMENTS

Note: At present the USNRC uses a modified earlier version (UDAD-IV) for licensing.

Note: The authors would appreciate comments and suggestions from readers, particularly those who use the code, regarding revisions that would make the code more useful and convenient.

M. Momeni
May 1, 1979

CONTENTS

CONTENTS

FIGURES

TABLES

THE URANIUM DISPERSION AND DOSIMETRY (UDAD) CODE

Michael H. Momeni, Y. C. Yuan and A. J. Zielen

1. INTRODUCTION

The projected increasing demand for uranium fuel for the generation of electricity has focused considerable public and regulatory attention on the potential impacts of processing natural uranium. The radiological impact of uranium extraction is associated primarily with uranium-238 and its radioactive daughters present in the ore (Fig. 1.1). Although uranium-235 is the principal component of uranium fuel production, its abundance in natural uranium is only 0.72 percent. Compared to the ^{238}U decay series, the ^{235}U series contributes negligibly to the quantity of radioactivity dispersed.

Figure 1.2 depicts the principal components of the Uranium Dispersion and Dosimetry (UDAD) Code. Pathways of exposure are through atmospheric dispersion of radioactivity, from the surface of the ground, and via the surface and groundwater. These pathways result in exposure by inhalation of radionuclides in the air, ingestion of contaminated food and water, as well as exposure to gamma radiation from contaminated ground and air.

The computer code, Uranium Dispersion And Dosimetry (UDAD), was developed to provide comprehensive estimates of the potential radiation dose rate and dose to the standard man and the standard population in the vicinity (80 km) of a uranium processing facility such as a uranium mill or mine. The UDAD Code was applied initially in 1976 for the assessment of the radiological impact of Bear Creek (NRC 1977) uranium mining and milling project and was later expanded for generic evaluation of uranium milling in the United States. Since 1976 it has been applied to review of several other uranium mills for licensing and radiological evaluation.

^{238}U (UI) 4.51 x 10^9 y	^{234}U (UII) 2.33 x 10^5 y

^{234}Pa (UX$_2$) 1.14 m
^{234}Pa (UZ) 6.7 h

β 99.85%
IT .15%

^{234}Th (UX$_1$) 24.5 d	^{230}Th (Io: ionium) 8.3 x 10^4 y

^{226}Ra ("radium") 1622 y

^{222}Em (Rn: radon) 3.825 d

^{218}At 1.3 s

β.03%

^{218}Po (Ra A) 3.05 m	^{214}Po (Ra C') 150 μs	^{210}Po (Ra F) 140 d

β 99.96%

β 100%

^{214}Bi (Ra C) 19.7 m	^{210}Bi (Ra E) 5.0 d

α 99.97%

^{214}Pb (Ra B) 26.8 m	^{210}Pb (Ra D) 22 y	^{206}Pb (Ra G) stable

α .04%

α 5 x 10^{-5} %

^{210}Tl (Ra C") 1.32 m	^{206}Tl (Ra E') 4.23 m
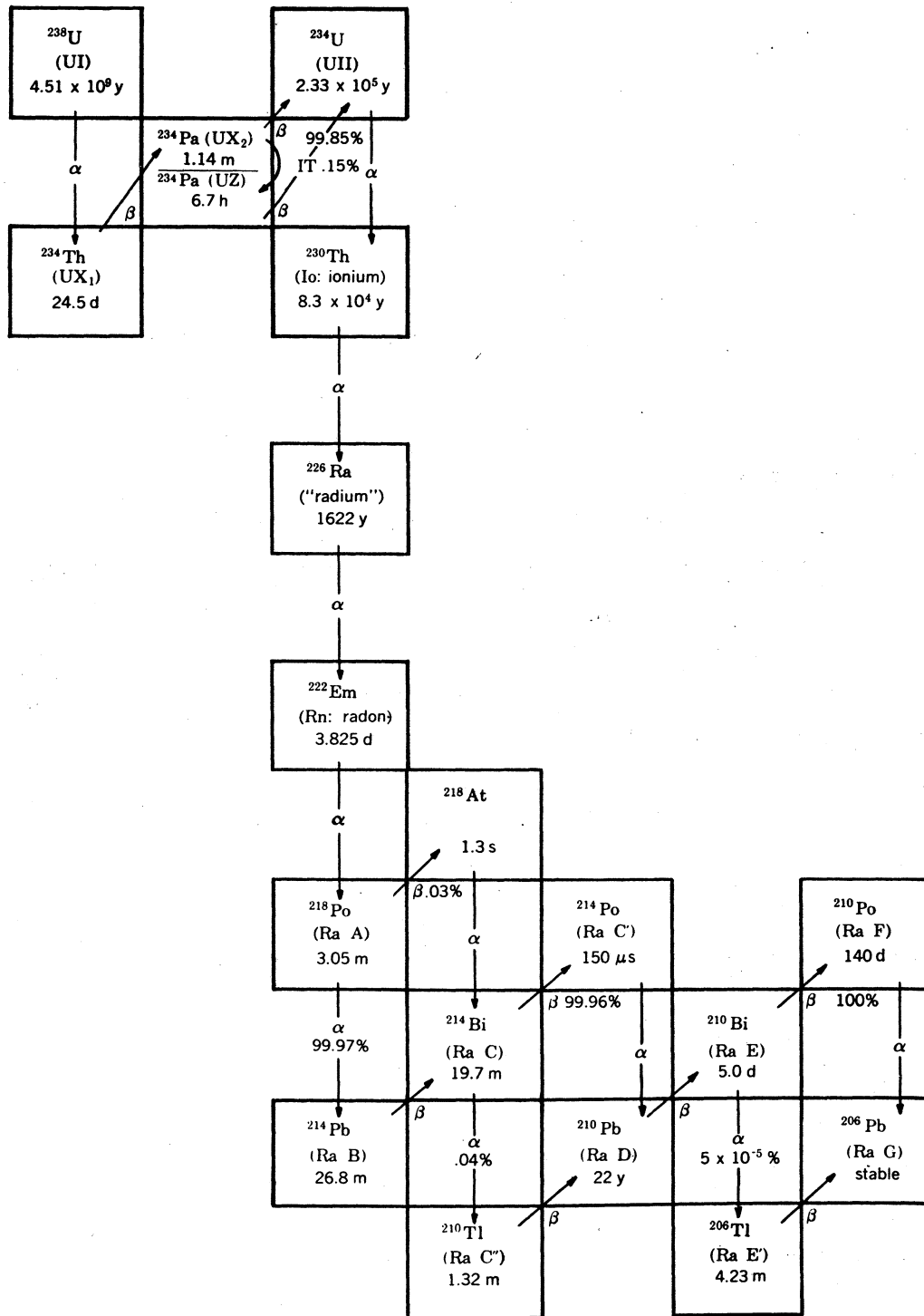
Fig. 1.1. The Uranium-238 Radioactive Decay Series.

UDAD

```
┌─────────────────────────────────────────┐
│ Source Term   Mining                     │
│               Transportation             │
│               Ore Storage                │
│               Ore Crushing and Grinding  │
│               Leaching and Extraction    │
│               Product Drying and Packaging│
│               Tailings                   │
└─────────────────────────────────────────┘
              │
         ┌──────────┐
         │Dispersion│
         └──────────┘
```

External Exposure   Internal Exposure

```
┌────────┐  ┌────────────┐  ┌────────────┐   ┌──────────┐  ┌──────────────────────┐
│ Direct │  │Contaminated│  │Contaminated│   │Inhalation│  │      Ingestion       │
│  from  │  │    Air     │  │    Soil    │   │          │  │                      │
│  Site  │  │            │  │            │   │          │  │  Water               │
└────────┘  └────────────┘  └────────────┘   └──────────┘  │  Meat                │
                                                           │  Grains              │
                                                           │  Fruits and Vegetables│
                                                           └──────────────────────┘
```

```
┌─────────────────────────┐          ┌───────────────────────────────────┐
│     Tissues at Risk     │          │        Tissues at Risk:           │
│  Whole Body             │          │  Bone                             │
│  Testes                 │          │  Bone Marrow                      │
│  Ovaries                │          │  Gastrointestinal Tract           │
│  Bone Marrow            │          │  Lung (nasopharynx, tracheobron-  │
│  Bone Cells             │          │  chial, pulmonary, and lymphoid   │
│  Lymphoid Tissues       │          │  tissues)                         │
│  Skin                   │          │                                   │
│  Gastrointestinal Tract │          │                                   │
└─────────────────────────┘          └───────────────────────────────────┘
```

```
┌──────────────────────────────────┐
│ Dose Rate and Dose to Tissues    │
│ at Risk, Population Exposure      │
│ and Environmental Dose Commitment │
└──────────────────────────────────┘
```

Fig. 1.2. The Uranium Dispersion and Dosimetry Code. External exposure by radiation directly from mines and mills and from the water from such facilities is not included in this code.

To assure consistency in the assessment methodology, a technical review group on radiological assessment for uranium mills was formed by the Nuclear Regulatory Commission (NRC) staff, the Environmental Protection Agency (EPA) and the Argonne National Laboratory (ANL) in early 1978 to discuss the detailed methodology for estimating dose rates, doses, and the environmental

dose commitment. A summary of the group's suggestions is given in Appendix F. The current version of the UDAD code (version IX) incorporates the recommendations of this review group.

In addition, parallel field investigations of dispersion pathways carried out by Argonne National Laboratory, Battelle Pacific Northwest Laboratory, and Environmental Protection Agency (Las Vegas) have further resulted in modification, reinforcement, and testing of the present model. Further modifications in the code and choices of the values for the default values are anticipated as these investigations are completed. Even though this code is dedicated to dispersion and dosimetry of uranium mining, milling, and fuel processing, it may be applied to the dispersion of any pollutants.

The model is written in Fortran IV and is designed for installation on an IBM 370/195 (or equivalent) computer. Substantial effort has been taken to reduce the computer core storage and to improve the computational efficiency. Application of this model will require a general purpose computer, certain input data, the instructions contained in this report, and the program itself. Based on individual needs, several options of the model can be eliminated with appropriate control of the input. Default values (Sec. 11) have been incorporated into the model based on NRC-EPA-ANL review group and USNRC staff suggestions (App. F). These default values may be replaced by site-specific data whenever such data are available.

In the following chapters, the contents of the model are described, and their formulation and intended uses are discussed. Chapter 11 describes the structure of the program and gives input instructions. A sample problem to assist in operation of the program is given in Chapter 12.

Reference for Section 1

U.S. Nuclear Regulatory Commission, *Final Environmental Statement, Bear Creek Project*, Office of Nuclear Materials Safety and Safeguards, Docket No. 40-8452, NUREG-0129, June 1977.

2. DISPERSION: STABLE GASEOUS POLLUTANTS

The atmospheric dispersion techniques incorporated in UDAD consist of a Gaussian plume dispersion model modified to include ground deposition, resuspension, and radioactive decay and daughter ingrowth. The model is designed to predict ground-level air concentration and surface contamination resulting from continuous release of uranium-238 and its decay products into the atmosphere from point releases or multiple area sources.

2.1 ATMOSPHERIC DISPERSION OF STABLE GASEOUS POLLUTANTS

Atmospheric dispersion of the radioactive materials occurs by transport and turbulent diffusion process. Methodologies for estimating concentrations of airborne materials transported directly from a point source to a receptor point have been outlined by Pasquill (1974) and Haugen (1975). For a large diffusion time and homogeneous stationary conditions the random transport of a stable pollutant may be stated in the form of the simple Fickian differential equation under the central limit theorem of statistics (Batchelor 1949, Cramer 1958, Barad 1959).

The average plume concentration from an instantaneous single ground-level release, assuming independent diffusion in the three cartesian coordinate directions $\hat{X}$, $\hat{Y}$, $\hat{Z}$, is described by:

$$\chi(x,y,z;i,j) = \frac{Q(i,j)(2\pi)^{-3/2}}{(\sigma_x \sigma_y \sigma_z)} \exp\left\{-\left[\frac{(x-\bar{u}t)^2}{2\sigma_x^2} + \frac{y^2}{2\sigma_y^2} + \frac{z^2}{2\sigma_z^2}\right]\right\}, \qquad (2.1)$$

where: χ is the atmospheric concentration of the stable gaseous pollutant i at location (x,y,z) relative to the source of emission j at coordinate $(0,0,0)$,

$Q(i,j)$ is the point source strength in curies,

6

σ^2_x, σ^2_y, σ^2_z are the variances of plume distribution in the directions $\hat{X}, \hat{Y}, \hat{Z}$, and

$\bar{u}$ is the average wind velocity in the direction of $\hat{X}$ diffused for a time period t reaching position (x,0,0).

The concentration of radioactivity from a ground-level source releasing activity at a continuous rate of Q´(Ci/sec) located at (0,0,0) is given by:

$$\bar{\chi}(x,y,z;i,j) = \frac{Q´(i,j)}{2\pi\sigma_y\sigma_z\bar{u}} \exp\left[-\left(\frac{y^2}{2\sigma^2_y} + \frac{z^2}{2\sigma^2_z}\right)\right] . \tag{2.2}$$

The diffusion along the $\hat{X}$ direction is practically negligible by comparison with the gross transport by the wind (Frenkiel 1953). Variances of plume distribution, σ^2_y and σ^2_z, are only functions of x. For the sources of release not at the earth's surface but at elevation h(j), the correction for ground reflection results in:

$$\bar{\chi}(x,y,z;i,j) = \frac{Q´(i,j,h)}{2\pi\sigma_y\sigma_z\bar{u}} \exp\left(-\frac{y^2}{2\sigma^2_y}\right) \times$$

$$\left\{\exp\left[-\frac{[z-h(j)]^2}{2\sigma^2_z}\right] + \exp\left[-\frac{[z+h(j)]^2}{2\sigma^2_z}\right]\right\} . \tag{2.3}$$

For the receptors located at (x,y,0), i.e., for ground-level concentration, Eq. 2.3 simplifies to:

$$\bar{\chi}(x,y,z=0;i,j) = \frac{Q´(i,j(h))}{\pi\sigma_y\sigma_z\bar{u}} \exp\left[-\left(\frac{y^2}{2\sigma^2_y} + \frac{h^2(j)}{2\sigma^2_z}\right)\right] . \tag{2.4}$$

Integration of Eq. 2.4 over the direction $\hat{Y}$ results in a crosswind integrated concentration $\bar{\chi}_c$:

$$\bar{\chi}_c(x,y,z=0;i,j) = \frac{Q´(i,j(h))}{\sqrt{\pi/2}\,\sigma_z\bar{u}} \exp\left(-\frac{h^2(j)}{2\sigma^2_z}\right) . \tag{2.5}$$

A practical problem associated with the radiological assessment of a uranium processing plant is that of estimating the average pollutant concentration over a long time period, such as one year. Since the wind velocity and

direction change over this long a period of time, the average concentration $\bar{\chi}_c$ must be normalized by the joint windspeed and direction frequency distribution. The concentration profile in the $\hat{Y}$ direction is assumed to be uniformly distributed over a sector. However, in a short time period the concentration will change as a result of changes in wind direction or intensity. The sector average ground-level concentration $<\chi(r,\theta,i,j)>$ in polar coordinates (r,θ) for a sector width $(2\pi r/n)$ from Eq. 2.5 is:

$$<\chi(r,\theta;i,j)> = \frac{nf(\theta)Q'(i,j)}{\pi\sqrt{2\pi}\,\sigma_z r\bar{u}} \exp\left[-\frac{h^2(j)}{2\sigma_z}\right],$$
(2.6)

where: f is the wind frequency,

n is the number of sectors, and

(r,θ) is the polar coordinate of the geometric center of the sector.

The above formulation, Eq. 2.6, implies a uniform crosswind concentration over the sector width, $2\pi r/n$, from the source j and in the vertical direction Gaussian in distribution and centered at the effective release height h(j). In UDAD n = 16 is used, which corresponds to $\Delta\theta$ = 22.5 degrees.

2.2 ATMOSPHERIC STABILITY

The variance, σ_z^2, in the $\hat{Z}$ direction is a function of atmospheric stability. Six stability categories used in this code are based on the criteria stated by Pasquill (1961). The standard deviation of the vertical distribution of concentration, σ_z, increases with the downwind distance. The values of σ_z adopted in this code are those of Briggs (1974) and Gifford (1976).

The standard deviation of the plume width in the vertical direction, σ_z, may be empirically expressed by:

$$\sigma_z(r,s) = a_s r\left(1 + b_s r\right)^{c_s},$$
(2.7)

where a, b, and c are the constants for each stability class s. The values for these constants were obtained empirically and are given in Table 2.1. Since Eq. 2.7 predicts unreasonable σ_z values for small distances r, the

Table 2.1. Stability Class Parameters* for Equation 2.7

Conditions	Pasquill Type Stability Class(s)	a	b	c
Extremely unstable	A	0.20	0.0	1.0
Moderately unstable	B	0.12	0.0	1.0
Slightly unstable	C	0.08	2×10^{-4}	-0.5
Neutral	D	0.06	1.5×10^{-3}	-0.5
Moderately stable	E	0.03	3×10^{-4}	-1.0
Very stable	F	0.016	3×10^{-4}	-1.0

*Briggs 1974 and Gifford 1976.

minimum distance allowed for Eq. 2.7 is 100 meters. For $r < 100$ m the σ_z value for $r = 100$ m is chosen.

2.3 ATMOSPHERIC DIFFUSION BOUNDARY

Vertical diffusion of pollutants is confined by the existence of stable atmospheric boundary at height ℓ. In UDAD the effects of mixing height are considered only for the unstable and neutral conditions (Table 2.1, classes A and D), as stable conditions limit the plume dispersion in the vertical direction. The standard deviation of the vertical distribution, σ_z, is predicted to increase in the downwind direction to a distance of r_1 at which $\sigma_z(r_1) = 0.47$ ℓ. At distance r_1 the concentration of pollutants at the base of the stable boundary layer will be one-tenth of the concentration at the plume center line.

For distances less than r_1, the concentration of the radioactivity in the vertical direction is assumed to be Gaussian in distribution. For distances greater than r_1 the effect of atmospheric trapping will increase with downwind distance. For distances greater than $2r_1$ the atmospheric concentration of the pollutant will be uniform below the mixing height ℓ. At these distances the concentration is calculated by:

$$<\chi(r;i,j)> = \frac{nfQ'(i,j)}{2\pi r \ell \bar{u}} .$$

$$(2.8)$$

For distances $r_1 < r < 2r_1$, the concentration is calculated by a linear interpolation between the Eqs. 2.6 and 2.8.

2.4 SEASONAL VARIATION OF MIXING BOUNDARY

The mixing layer height ℓ varies greatly between seasons, from day to day, and diurnally. Since accounting for all variations of ℓ is not practical in these computations, an annual average mixing layer $<\bar{\ell}>$ may be calculated from either:

$$\frac{1}{<\ell>} = \frac{1}{2}\left(\frac{1}{\bar{\ell}_1} + \frac{1}{\bar{\ell}_2}\right)$$

or

$$<\bar{\ell}> = w_1 l_1 + w_2 l_2 . \tag{2.9}$$

where $\bar{\ell}_1$ and $\bar{\ell}_2$ are, respectively, the annual average morning and afternoon mixing heights, l_1 and l_2 are maximum and minimum annual average diurnal mixing heights, and w_1 and w_2 are weight factors. The average, $<\bar{\ell}>$, is inputed in the code.

2.5 WIND SPEED AND WIND DIRECTION

Wind speeds are assumed to be piecewise constant and are grouped in six classes. Wind directions are grouped into 16 compass angles of 22.5° circular sectors. The discontinuities at the sector boundaries which are created by the sector average approximation are smoothed using a linear interpolation of concentrations between the receptor sector and the adjacent sectors. For a point $P(r,\theta)$ located between two sectors θ_1 and θ_2 ($\theta_1 \leq \theta \leq \theta_2$) the concentration is computed by:

$$<\chi(r,\theta;i,j)> = \left(\frac{SW - C_1}{SW}\right) <\chi(r,\theta_1;i,j)> + \left(\frac{SW - C_2}{SW}\right)<\chi(r,\theta_2;i,j)> , \tag{2.10}$$

where SW is the sector width at the receptor distance r, i.e., $SW = 2\pi r/n$, and C_1 and C_2 are the crosswind distances between the receptor and sectors defined by adjacent centerline angles θ_1 and θ_2.

2.6 PLUME RISE

Plume rise above the height of the source is a function of the effluent exit momentum, thermal buoyancy and the effect of molecular weight difference between the effluent and the ambient air. In UDAD the height of rise of an effluent (Δh) (Holland 1953) is given by:

$$\Delta h = \frac{1.5 \ Vd}{\bar{u}} \qquad (2.11)$$

where: d is the stack diameter (meters), and

V is the efflux velocity (meters/second).

The thermal buoyancy term in the original formula is omitted from the above equation since for the uranium mill stacks its contribution is generally negligible compared to that of the momentum term.

2.7 AREA SOURCES

Not all sources of emission are point sources, such as uranium product dryer stacks. Other sources are large in extent and cannot be approximated as point sources for near receptors; for example, tailing retention areas and ore pads.

Large, irregular sources of area A are subdivided into smaller areas $a = A/m$. UDAD converts each source area "a" into either squares of width "d" or rectangles. A "virtual point source" is assumed to be located a distance of d/z cot ($\Delta\theta/2$) upwind from the center of the source area. $\Delta\theta$ is the sector angle of 22.5 degrees used to subtend the area width. For those receptors which cannot observe the emission from the total of the source area within the 22.5-degree sector, a multiplicative correction factor is generated. This factor is the ratio of that portion of the source area within the 22.5-degree sector located upwind from the receptor to that of the total source area.

2.8 ANNUAL AVERAGE CONCENTRATION

The annual average concentration $<\chi(r,\theta;i)>$ for pollutant i from all sources j and representative windspeeds and directions is calculated from

$$<\chi(\vec{r};i)> = \sum_j \sum_W \sum_D \sum_S f(W,D,S)\bar{\chi}(\vec{r} - \vec{r}(j),\theta,W,D,S) \, , \qquad (2.12)$$

where $f(W,D,S)$ is the normalized frequency for wind-sector direction D, the windspeed class W, and stability category S. $\bar{\chi}(\vec{r}-\vec{r}(j),W,D,S)$ is the contribution of source j located at $\vec{r}(j)$ to the concentration at receptor located at (r,θ) given by vector $\vec{r}$.

References for Section 2

Barad, M. L., and D. A. Haugen, *A Preliminary Evaluation of Sutton's Hypothesis for Diffusion from a Continuous Point Source*, J. Meteorol. 16(1):12-20, 1959.

Batchelor, G. K. *Diffusion in a Field of Homogeneous Turbulence. I. Eulerian Analysis*, Australian J. Sci. Res. 2:437-450, 1949.

Briggs, G. A., *Diffusion Estimation for Small Emissions*, in Environmental Research Laboratories Air Resources Atmosphere Turbulence and Diffusion Laboratory 1973 Annual Report, USAEC Report ATDL-106, National Oceanic and Atmospheric Administration, December 1974.

Cramer, H. E., F. A. Records, and H. C. Vaughan, *The Study of the Diffusion of Gases or Aerosols in the Lower Atmospheric*, Report AFCRC-TR-58-239, Department of Meteorology, Massachusetts Institute of Technology, 1958.

Frenkiel, F. N., *Turbulent Diffusion: Mean Concentration Distribution in a Flow Field of Homogeneous Turbulence*, Advan. Appl. Mech., 3:61-107, 1953.

Gifford, F. A., *Turbulent Diffusion-Typing Schemes: A Review*, Nuclear Safety, v. 17-1, Jan.-Feb. 1976.

Haugen, D. A., Lectures on Air Pollution and Environmental Impact Analysis, American Meteorological Society, Boston, 1975.

Holland, J. Z., *A Meteorological Survey of the Oak Ridge Area: Final Report Covering the Period 1948-52*, USAEC Report ORO-99, Weather Bureau, Oak Ridge, Tennessee, 1953.

NTIS, Air Quality Display Model, National Technical Information Service, 1969.

12

Pasquill, F., *The Estimation of Windborne Material*, Meteorological Magazine 90:33-49, 1961.

Pasquill, F., *Atmospheric Diffusion*, 2nd Ed., Halsted Press, New York, 1974.

Turner, D. B., *A Diffusion Model of an Urban Area*, J. Appl. Meteorology, Feb. 1964.

3. AIRBORNE TRANSIT RADIOACTIVE DECAY

Radioactive decay and the ingrowth of radionuclides during the transit time that elapses as materials disperse from a source to a receptor are discussed in this section.

3.1 RADIOACTIVE DECAY AND INGROWTH

In the previous chapters the expressions for the atmospheric dispersion did not consider radioactive decay and ingrowth. Radioactive pollutants [238]U, [234]U, [230]Th, [226]Ra, ^{210}Pb, and [210]Po are sufficiently long-lived so that the transit time from the source to the 80-km distance considered in this code does not result in any detectable decay (<0.0001%). Thus, radioactive decay and ingrowth do not affect the concentrations of these radionuclides in the atmosphere. In UDAD, the decay and ingrowth of the short-lived radon ([222]Rn) and its daughters ([218]Po, [214]Pb, and [214]Bi) are calculated. The transit time τ during which radioactive decay occurs may be approximated by the ratio of the distance r traveled to the windspeed u, i.e., $\tau = r/u$. The radon source strength Q' (radon, j) may be corrected for radioactive decay by:

$$Q'(r,\theta;radon,j) = Q'_0(radon,j) \exp\left(-\frac{0.693\ \tau}{T_1}\right) \tag{3.1}$$

where T_1 is the radioactive half-life (3.82 days) of radon-222.

The ingrowth of radon daughters is dependent on the radioactive half-lives (Table 3.1) and transit time. The concentration of radon daughters in the air is given by:

$$\chi_n(r) = \chi_1(r)\left(\prod_{i=2}^{n}\frac{0.693}{T_i}\right)\left\{\sum_{i=1}^{n}\left[\frac{\exp(-0.693\ r/T_i u)}{\prod_{\substack{j=1\\j\neq i}}^{n}0.693\left(\frac{1}{T_j}-\frac{1}{T_i}\right)}\right]\right\} \tag{3.2}$$

for n = 2,...7

Table 3.1. Radioactive Half-Life of Radon and Its Daughters

Radionuclide	Half-Life	n	E_n (MeV)	$L_n \times 10^6$ (WL/pCi/m^3)
^{222}Rn	3.82 days	1	5.49	---
$\downarrow \alpha$				
^{218}Po	3.05 minutes	2	6.00	1.03
$\downarrow \alpha$				
^{214}Pb	26.8 minutes	3	---	5.07
$\downarrow \beta$				
^{214}Bi	19.7 minutes	4	---	3.73
$\downarrow \beta$				
^{214}Po	10^{-6} minutes		7.68	a/
$\downarrow \alpha$				
^{210}Pb	22 years	5	---	---
$\downarrow \beta$				
^{210}Bi	5 days	6	---	---
$\downarrow \beta$				
^{210}Po	143 days	7	---	---

[a] A negligible contribution.

where i is the ith daughter radionuclide (Table 3.1). For lead-210 and polonium-210 produced from radon in transit, a deposition velocity of $V_d = 0.003$ m/sec is assumed (see Sec. 4.2).

3.2 WORKING LEVEL

Concentrations of short-lived radon daughters are sometimes expressed in working levels (WL) units. One "working level" is defined as any combination of short-lived radon daughters in one liter of air that will result in the ultimate emission of 1.3×10^5 MeV of alpha energy. Working levels in UDAD are calculated from

$$WL(r,\theta) = \sum_{n=2}^{4} L_n \chi_n(r,\theta) \tag{3.3}$$

where χ_n is nth (Table 3.1) radon daughter concentration in air calculated from Eq. (3.2) and L_n is the working level conversion factor of radon daughter n. Based on the definition of working level, L_n is given by:

$$L_n = \frac{3.7 \times 10^{-5} \sum_{j=n}^{4} E_n(\alpha)}{1.3 \times 10^5 \lambda_n} \tag{3.4}$$

or

$$L_n = \frac{2.846 \times 10^{-10}}{\lambda_n} \sum_{j=n}^{4} E_n(\alpha) \quad \frac{WL}{pCi/m^3} \tag{3.5}$$

where $E_n(\alpha)$ is the potential alpha energy for the nth radon daughter (Table 3.1).

4. DISPERSION: PARTICULATE POLLUTANTS

Dispersion of polydisperse pollutants emitted into the atmosphere may be altered by deposition of the airborne material upon the surface of the ground. The mechanisms of deposition include gravitational settling (fallout), precipitation scavenging (washout), surface impaction, electrostatic attraction and adsorption. Deposition and resuspension are dependent on the physical characteristics of the pollutants in addition to the wind strength and surface characteristics and topography. Even though other processes contribute to plume depletion, our attention has been focused on dry deposition.

4.1 PARTICULATE CHARACTERISTICS

By and large, the size, density and shape of particles are primary factors which determine the behavior of the airborne particulates. The size distribution of particles in the atmosphere is not constant and may change with altitude and atmospheric conditions. Although polydisperse particles in atmosphere have a continuous size distribution, in the "standard UDAD" (Version IX) the physical size distributions of particulates are entered using a class of five sizes along with pollutant density. Size distribution is entered individually for each source.

4.2 GROUND DEPOSITION AND SETTLING

Physical processes controlling deposition on the ground are not well understood. The deposition rate $\dot{W}_s$ has been empirically defined by (Chamberlain 1953):

$$\dot{W}_s = <\chi(s)>V_d(s) \ . \tag{4.1}$$

Since deposition rate is a function of size s, integration over all sizes results in:

$$\dot{W} = \int <\chi(s)> V_d(s) \ ds \ . \tag{4.2}$$

where $<\chi(s)>$ is a time-averaged atmospheric concentration of a pollutant of size s and deposition velocity $V_d(s)$.

Airborne particulates of diameter d_p in the gravitation force F and with friction coefficient f experience a terminal settling or drift velocity V_s given by:

$$V_s = \frac{F}{f} \ . \tag{4.3}$$

The gravitational field force F is given by:

$$F = \frac{\pi d_p^3}{6} (\rho_p - \rho)g \ , \tag{4.4}$$

where ρ and ρ_p are the gas and particle densities, respectively, and g is acceleration due to gravity. f is given by the Stokes law for friction resistance at low Reynolds numbers (R<1.0):

$$f = 3\pi\mu d_p/C \ , \tag{4.5}$$

where μ is the dynamic atmospheric viscosity and C is the slip correction factor. Thus:

$$V_s = \left[\frac{\pi d_p^3}{6} (\rho_p - \rho)g\right] \Big/ (3\pi\mu d_p/C) \ ,$$

$$V_s = \left[\frac{d_p^2 g(\rho_p - \rho)C}{18\mu}\right] \ ,$$

$$V_s = \frac{\rho_p g d_p^2 C}{18\mu} \left[1 - \frac{\rho}{\rho_p}\right] \cong \frac{\rho_p g d_p^2 C}{18\mu} \ . \tag{4.6}$$

Usually ρ/ρ_p can be neglected in the above equation. The values for the slip correction factor (Davies 1945) are given in Table 4.1. For particles $d_p > 5$ μm, the slip correction factor is about unity. Thus, the settling velocity is calculated from:

$$V_s = 3 \times 10^{-5} d_p^2 \rho_p C , \qquad\qquad (4.7)$$

where V_s, d_p, and ρ_p are in m/sec, μm and g/cm^3, respectively. The default value for C is unity, but other values than the C = 1 can be inputed into Eq. 4.7 through NAMELIST (see Sec. 11).

Table 4.1. Depositional* Properties of Spherical Particles with Density 1 g/cm^3 at 20°C and One Atmospheric Pressure

Particle Diameter, μm	Slip Correction Factor	V_s, cm/sec
0.05	5.0	
0.1	2.9	8.6×10^{-5}
0.2	1.9	2.3×10^{-4}
0.5	1.3	1.0×10^{-3}
1.0	1.2	3.5×10^{-3}
2.0	1.1	1.3×10^{-2}
5.0	1.0	7.8×10^{-2}
10.0	1.0	3.1×10^{-1}
20.0	1.0	1.2
50.0	1.0	7.6
100.0	1.0	30.3

*Friedlander 1977.

For fall velocities less than 1 cm/sec the vertical movement of the particle is largely dependent on the vertical turbulence and mean motion of the air, and the contribution from particle sedimentation is small. In the range where the sedimentation rate is significant (V_s = 1 to 100 cm/sec), the vertical distribution of particle concentration in the plume may be expressed by a variable effective plume height based on "tilting plume model":

$$h(r) = [h(0) - h_1(r)] - \frac{rV_s}{\bar{u}} \qquad \text{for } h(r) \geq 0 , \qquad (4.8)$$

where $h_1(r)$ is the ground elevation at downwind distance r.

Deposition velocity is a function of wind velocity in addition to particle size (Sehmel 1971). For particles with settling velocities $V_s \leq 0.01$ m/sec, UDAD used a deposition velocity $V_d = 0.01$ m/sec. For particles with $V_s > 0.01$ m/sec, the deposition velocity is assumed to be equal to the calculated settling velocity. For radon daughters, $V_s = 0.003$ m/sec is assumed.

Depletion of the plume by the process of settling and deposition discussed above results in decreased concentration at receptor locations at increasing distances from the point of release. Chemberlain (1953) modified the source term to correct for deposition to a reduced (depleted) source term to account for the observed decreased concentration. In UDAD the effective source strength Q(r) at a downwind distance r from the source Q(0) at r = 0 was derived from:

$$Q(r) = Q(0) \exp\left[(-V_d/u)F_1(0,r)\right] \qquad \text{for } r \leq r_\ell , \qquad (4.9)$$

$$Q(r) = Q(0)\left\{-\left(\frac{V_d}{u}\right)\left[F_1(0,r_\ell) + F_2(r_\ell,r) + \frac{(r - r_\ell)^2}{2r_\ell \ell}\right]\right\}$$

$$\text{for } r_\ell < r \leq 2r_\ell , \qquad (4.10)$$

$$Q(r) = Q(0)\left\{-\left(\frac{V_d}{u}\right)\left[F_1(0,r_\ell) + F_2(r_\ell,2r_\ell) + \frac{r_\ell}{2\ell} + \frac{r - 2r_\ell}{\ell}\right]\right\}$$

$$\text{for } r > 2r_\ell , \qquad (4.11)$$

20

$$\text{where } F_1(r_1, r_2) = \int_{r_1}^{r_2} \left\{ \exp\left[-\frac{1}{2}\left(\frac{h}{\sigma_z}\right)^2\right] \Big/ \sigma_z \right\} dr$$

$$\text{and} \quad F_2(r_1, r_2) = \int_{r_1}^{r_2} \left\{ \exp\left[-\frac{1}{2}\left(\frac{h}{\sigma_z}\right)^2\right] (2r_\ell - r)/\sigma_z r_\ell \right\} dr \ .$$

These integrals are evaluated numerically in the program based on the fourth Newton-Cotes formula (Hillstrom 1968).

4.3 FUGITIVE DUST AND WIND EROSION

The mechanism of movement of particles from a contaminated area is dependent on wind velocity, soil properties, and the nature of the surface. Wind forces can generate three basic modes of particulate movement: surface creep, saltation, and airborne suspension. Surface creep involves particles ranging in size from 500 to 1000 μm. These particles are rolled along the surface by the push of strong winds and by exchange of momentum after impact with smaller particles in saltation. Saltation consists of individual particles jumping and lurching within a few centimeters of the ground. Particles that saltate are from 100 to 500 μm in size, depending on shape and density, and are quickly brought back to the ground by the gravitational force. Particles smaller than 100 μm may have a fall velocity lower than the upward velocity of the turbulent wind. Such particles are carried through the atmosphere for long periods and to great distances from their original location. The mechanism by which fine particles are lifted off the ground is different from that of saltation. It has been observed that samples of soil composed only of fine dust particles were extremely resistant to erosion by wind (Chepil 1945). In mixtures with coarser grains, however, these particles moved readily. It was concluded that suspension of fine dust in air is mainly the result of movement of grains in saltation.

The wind velocity profile near the surface can be described by the general equations (Bagnold 1941):

$$U* = (\tau/\rho)^{\frac{1}{2}} \quad \text{or} \tag{4.12}$$

$$U* = \frac{U_z}{2.5 \ln (z/z_0)} \tag{4.13}$$

where $U*$ is the shear velocity

        τ is the surface shear stress,

        ρ is the density of air,

        z is the height above surface,

        U_z is the wind velocity at height z, and

        z_0 is the surface roughness height.

When the velocity of the wind along the surface exceeds a threshold, particle saltation begins. The initiation of saltation of particles has been investigated by Bagnold (1941), who obtained the following expression for the threshold value of the shear velocity, U_t^*:

$$U_t^* = A\sqrt{\frac{\alpha - \rho}{\rho} gd} \tag{4.14}$$

where α is the density of the grain,

        ρ is the density of air,

        g is the gravitational constant,

        d is the diameter of the grain, and

        A is the dimensionless coefficient of 0.1 in value.

The influence of moisture in the sand on the threshold velocity for grain movement has been investigated by Belly (1964). Based on his study, Eq. 4.14 may be modified as follows:

$$U_t^* = A\sqrt{\frac{\alpha - \rho}{\rho} gd}\ (1.8 + 0.6 \log_{10} W)\ , \tag{4.15}$$

where W is the water content expressed in weight by percent. In UDAD, for dry surface the default value for moisture is 0.1%.

The rate of horizontal particle movement by the saltation process in mass per unit width and unit time, q, was found by Bagnold to vary directly as the cube of the surface shear velocity (Bagnold 1941):

$$q = C_h \cdot U*^3 \ , \tag{4.16}$$

where C_h is a constant dependent on the soil and surface conditions.

A modified relationship, proposed by Lettan and reported by Gillette (1973), for the horizontal flux was reported for various soil types under similar erosion conditions. This modification of Eq. 4.16 is given by:

$$q = CU*^2 (U* - U*_t), \text{ for } U* > U*_t \ , \tag{4.17}$$

and

$$q = 0 \text{ for } U* \leq U*_t \ , \tag{4.18}$$

where the shear velocities $U*$ and $U*_t$ have units of cm/sec, the horizontal flux q has units of g/cm-sec, and C is 10^{-6}.

The wind pickup of fine particulate material (diameter $d \leq 20$ μm) from the soil surface has been investigated by Gillette (1973). He found that the vertical flux, expressed in mass per unit area and unit time, Φ^v_{20}, obeyed the empirical formula:

$$\Phi^v_{20} = C_v \left(U* \big/ U*_t \right)^\eta \ , \tag{4.19}$$

where the coefficient of proportionality C_v is about 2×10^{-10}, and η is a constant dependent on the fraction of the fine particles in the soil.

Since vertical fluxes are never observed without horizontal fluxes, an assumption was made that for wind-eroding surfaces, the vertical flux is directly proportional to q. Travis (1974) derived the following relationship:

$$\Phi^v_{20} = q \left(\frac{C_v}{U*_t^3 \, C_h} \right) \left(\frac{U*}{U*_t} \right)^{\eta - 3} \ , \tag{4.20}$$

where η is greater than three and **increases** as the number of suspendable particles per unit mass increases.

A linear curve fitting by Travis (1974) of Gillette's experimental field data for η as a function of the particle mass percentage less than 20 μm in diameter, p, yields the expression:

$$\eta = (p/3) + 3 \ . \tag{4.21}$$

Since the vertical flux must tend to zero as the suspended particle mass percentage p approaches zero, Eq. 4.20 was modified as follows:

$$\Phi_{20}^{V} = q \left(\frac{C_v}{U_t^* \, C_h} \right) \left[\left(\frac{U^*}{U_t^*} \right)^{(p/3)} - 1 \right] \ . \tag{4.22}$$

The constants C_v and C_h were given by Gillette (1973) as approximately 2×10^{-10} and 10^{-6}, respectively.

For the particulate material having a diameter $d \leq 100$ μm in UDAD the total vertical flux Φ^V for radionuclide i, in activity, is estimated from:

$$\Phi^V(i) = \frac{\Phi_{20}^V \, I_{20}(i)}{F_{20}} \tag{4.23}$$

where $I_{20}(i)$ is specific activity of radionuclide i in the contaminated area with $d \leq 20$ μm; F_{20} is the activity fraction of suspended particles that are less than 20 μm in diameter. For each wind speed class, the release of radioactive particulates from a contaminated area is calculated for the average wind speed. The annual release of particulates is obtained from the contributions from each wind speed class.

The default values in UDAD for estimation of particulate flux from tailings piles in lieu of actual measurements are:

        Surface roughness height $z_0 = 1$ cm,

        Density of the tailings grains $\alpha = 2.4$ g/cm^3,

        Average grain diameter $d = 300$ μm, and

        Percent of tailing mass that has a diameter smaller than 20 μm,

          $p = 3.0$

Activity fraction of $d \leq 20$ µm is $F_{20} = 0.4$.

4.4 RESUSPENSION CONCENTRATION

Particulate material deposited on the ground may re-enter the atmosphere by resuspension processes. The concentrations of resuspended particulates in the air are dependent on many environmental factors, such as the geometrical configuration of the land surface, the meteorological conditions, the characteristics of the deposited particulates, the parameters of the soil and the vegetation cover, the disturbance of contamination surfaces by human activity, and the time since deposition. The time factor is necessary to include the weathering processes which alter the physical and chemical states of the contaminant, attachment to host soil particles, downward migration through the soil profile by physical and chemical processes, and loss from the site.

The resuspension factor has been measured under a variety of conditions. For freshly deposited contaminants, the resuspension factor has been found to vary between 10^{-7}/m and 10^{-3}/m. For aged contaminants the resuspension factor is of the order of 10^{-9}/m.

On a contaminated surface, two processes may be assumed to contribute to the net interchange of material between the ground and the air--resuspension and deposition. The net surface flux from a contaminated surface to the air is:

$$F_z(x,y) = -V_d \chi(x,y) + \Lambda W(x,y) , \qquad (4.24)$$

where V_d is the deposition velocity (m/sec),

Λ the resuspension rate (sec^{-1}),

χ the air concentration (activity/m^3), and

W the surface contamination per unit area (activity/m^2).

For the conservative case of no weathering and in a steady-state condition of a uniformly distributed infinite contamination, the net flux is zero. Thus, the resuspension factor:

$$K = \chi/W \ , \tag{4.25}$$

can be expressed in terms of resuspension rate and deposition velocity:

$$K = \Lambda/V_d \ . \tag{4.26}$$

The resuspension rate, Λ, is the fraction resuspended from the surface per second and is highly dependent on the wind speed and the deposition surface. At heights near to the ground because of absence of experimental data, Λ is assumed to be independent of particle size. Thus:

$$\frac{K(d_1)}{K(d_2)} = \frac{V_d(d_2)}{V_d(d_1)} \ . \tag{4.27}$$

For small particles (d < 10 μm) with deposition velocity of 0.01 m/sec and assuming a resuspension factor of 10^{-5}/m, the resuspension factor for a 35-μm diameter particle size can be estimated as:
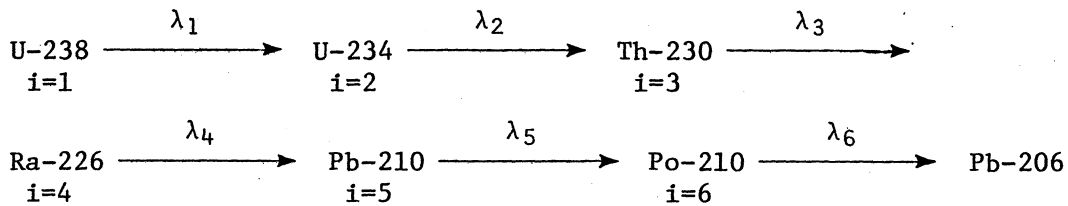
$$K(d=35\mu m) = \frac{10^{-5} \times 0.01}{0.0882} = 1.14 \times 10^{-6}/m \tag{4.28}$$

The resuspension factor is time dependent, and in UDAD the concentration from resuspension, $<\chi^R(r,\theta,t)>$, is expressed as:

$$<\chi^R(r,\theta,t)> = W(r,\theta,t)K(0) \ \exp \ (-\omega t) \tag{4.29}$$

where $W(r,\theta,t)$ is the surface contamination activity,

ω is the weathering process coefficient, and

$K(0)$ is the initial resuspension factor.

An estimate of the weathering process half-time is between 35 to 70 days. In UDAD, we have assumed that the default initial value of $K(0) = 10^{-5}$/m will diminish with a weathering half-time of 50 days (default value) to $K_f = 10^{-9}$/m (default value) after a period of 1.82 years. This time the resuspension factor would remain constant. Radionuclides considered for resuspension in UDAD are those with long radioactive half-lives:

26

$$
\begin{array}{cccc}
\text{U-238} \xrightarrow{\quad \lambda_1 \quad} & \text{U-234} \xrightarrow{\quad \lambda_2 \quad} & \text{Th-230} \xrightarrow{\quad \lambda_3 \quad} \\
i=1 & i=2 & i=3
\end{array}
$$

$$
\begin{array}{cccc}
\text{Ra-226} \xrightarrow{\quad \lambda_4 \quad} & \text{Pb-210} \xrightarrow{\quad \lambda_5 \quad} & \text{Po-210} \xrightarrow{\quad \lambda_6 \quad} & \text{Pb-206} \\
i=4 & i=5 & i=6
\end{array}
$$

The estimated surface contamination includes buildup of daughter products.

Resuspension radionuclide concentration $\langle\chi^R(r,\theta,t;s,i)\rangle$ for radionuclide i of particle size s is proportional to the initial plume concentration $\langle\chi(r,\theta;s,h)\rangle$:

$$
\langle\chi^R(r,\theta,t;s,i)\rangle = \sum_{h=1}^{i} \Bigg\{ K(0)\langle\chi(r,\theta;s,h)\rangle V_d(s,h)
$$

$$
\left(\prod_{\nu=h+1}^{i} \lambda_\nu \right) \sum_{\nu=h}^{i} \left[\frac{1 - \exp\left[-(\lambda_\nu + \mu + \omega)t\right]}{(\lambda_\nu + \mu + \omega) \prod_{\substack{f=h \\ f\neq\nu}}^{i} (\lambda_f - \lambda_\nu)} \right] \Bigg\} \qquad (4.30)
$$

for $t \leq t_a$,

where ν and h are radionuclides in the chain of U-238 series (i=1,2...6) above,

λ_ν is the radioactive decay coefficient,

μ is the effective removal constant from the ground (denudation coefficient),

ω is the weathering process coefficient for the resuspension factor, and

t_a = 1.8 years.

For periods $t_a < t < t_e$, where t_e is the duration of continuous release (for example, a mill operation period), $\beta_\nu = \lambda_\nu + \mu + \omega$, and $\alpha_\nu = \lambda_\nu + \mu$,

$$\langle \chi^R(r,\theta,t;s,i)\rangle = \sum_{h=1}^{i} k(0)\langle \chi(r,\theta;s,h)\rangle V_d(s,h)$$

$$\left(\prod_{\nu=h+1}^{i} \lambda_\nu\right) \sum_{\nu=h}^{i} \left[\frac{1 - \exp(-\beta_\nu t_a)}{(\beta_\nu)\prod_{\substack{f=h \\ f\neq\nu}}^{i}(\lambda_f - \lambda_\nu)}\right] +$$

$$\sum_{h=1}^{i} \left\{ k_f\langle \chi(r,\theta;s,h)\rangle V_d(s,h)\left(\prod_{\nu=h+1}^{i} \lambda_\nu\right)\sum_{\nu=h}^{i} \left[\frac{\exp(-\alpha_\nu t_a) - \exp(-\alpha_\nu t)}{\alpha_\nu \prod_{\substack{f=h \\ f\neq\nu}}(\lambda_f - \lambda_\nu)}\right]\right\} \tag{4.31}$$

For $t_e < t \leq t_e + t_a$:

$$\langle \chi^R(r,\theta,t;s,i)\rangle = \sum_{h=1}^{i} \left\{ k_0\langle \chi(r,\theta;s,h)\rangle V_d(s,h)\left(\prod_{\nu=h+1}^{i} \lambda_\nu\right)\right.$$

$$\left.\sum_{\nu=h}^{i} \left[\frac{\exp[-\beta_\nu(t - t_e)] - \exp(-\beta_\nu t_a)}{\beta_\nu \prod_{\substack{f=h \\ f\neq\nu}}^{i}(\lambda_f - \lambda_\nu)}\right]\right\} +$$

$$\sum_{h=1}^{i} \left\{ k_f\langle \chi(r,\theta;s,h)\rangle V_d(s,h)\left(\prod_{j=h+1}^{i} \lambda_\nu\right)\sum_{\nu=h}^{i} \left[\frac{\exp(-\alpha_\nu t_a) - \exp(-\alpha_\nu t)}{\alpha_\nu \prod_{\substack{f=h \\ f\neq\nu}}^{i}(\lambda_f - \lambda_\nu)}\right]\right\} . \tag{4.32}$$

For the period $t \geq t_e$ after operation:

$$\langle \chi^R(r,\theta,t;s,i)\rangle = \sum_{h=1}^{i} \left\{ k_f\langle \chi(r,\theta;s,h)\rangle V_d(s,h)\right.$$

$$\left.\left(\prod_{\nu=h+1}^{i} \lambda_\nu\right)\sum_{\nu=h}^{i} \left[\frac{\exp[-\alpha_\nu(t - t_e) - \exp(-\alpha_\nu t)]}{\alpha_\nu \prod_{\substack{f=h \\ f\neq\nu}}^{n}(\lambda_h - \lambda_\nu)}\right]\right\} . \tag{4.33}$$

4.5 CONCENTRATION OF RADIONUCLIDES ON THE GROUND

The calculated concentrations of each radionuclide on the ground includes buildup from continuous deposition and ingrowth of radioactive daughters, radioactive decay and weathering processes.

The time-dependent concentration of each radionuclide on the ground $W(r,\theta,t,i)$ for $t \le t_e$ is given by:

$$W(r,\theta,t;i) = \sum_{s=1} \sum_{h=1}^{i} \left\{ <\chi(r,\theta;s,h)>V_d(s,h) \left(\prod_{\nu=h+1}^{i} \lambda_\nu \right) \right.$$

$$\left. \sum_{\nu=h}^{i} \left[\frac{1 - \exp(-\alpha_\nu t)}{\alpha_\nu \prod_{\substack{f=h \\ f\neq\nu}}^{i} (\lambda_f - \lambda_\nu)} \right] \right\} , \tag{4.34}$$

where $\alpha_\nu = \lambda_\nu + \mu$.

For $t > t_e$ the concentration is:

$$W(r,\theta,t;i) = \sum_{s=1} \sum_{h=1}^{i} \left\{ <\chi(r,\theta;s,h)>V_d(s,h) \left(\prod_{\nu=h+1}^{i} \lambda_\nu \right) \right.$$

$$\left. \sum_{\nu=h}^{i} \left[\frac{\exp[-\alpha_\nu(t - t_e)] - \exp(-\alpha_\nu t)}{\alpha_\nu \prod_{\substack{f=h \\ f\neq\nu}}^{i} (\lambda_f - \lambda_\nu)} \right] \right\} . \tag{4.35}$$

References for Section 4

Bagnold, P. A., *The Physics of Blown Sand and Desert Dunes*, Methuen and Co., Ltd., London, 1941.

Belly, P., *Sand Movement by Wind*, Defense Documentation Center for Scientific and Technical Information, January 1964.

Chamberlain, A. C., *Aspects of Travel and Deposition of Aerosol and Vapor Clouds*, British Report AERE-HP/R-1261, 1953.

Chepil, W. S., *Dynamics of Wind Erosion*, Soil Sci 60, 1945.

Davies, C. N., Proc. Physical Society 57:259, 1945.

Friedlander, S. K., *Smoke, Dust and Haze*, in "Fundamentals of Aerosol Behavior," John Wiley & Sons, 1977.

Gillette, D. A., *On the Production of Soil Wind Erosion Aerosols Having the Potential for Long Range Transport*, Special Issue of Journal de Recherches Atmospherique on the Nice Symposium on the Chemistry of Sea-Air Particulate Exchange Processes, Nice, France, October 1973.

Hillstrom, K., *ANC4, 05/360 Fortran IV Routine for Adaptive Quadrature Using the Fourth Newton-Coles Formula*, ANL-D158,S, Argonne National Laboratory, April 1968.

Sehmel, G. A., *Particle Diffusivities and Deposition Velocities over a Horizontal Smooth Surface*, J. Colloid and Interface Sci, 37:891-906, 1971.

Travis, J. R., *A Model for Predicting the Redistribution of Particulate Contaminants from Soil Surface*, Atmospheric-Surface Exchange of Particulate and Gaseous Pollutants, CONF-740921, September 1974.

5. DOSIMETRY

Potential radiological effects of dispersed effluents to an individual are dependent on the dose rate and dose, age at exposure, and sex. Dose rate (rate of absorption of radiation energy) to an organ is dependent on the pathways of exposure to the pollutants. In UDAD, pathways of exposure (Fig. 1.2) are divided broadly into external and internal routes. External exposure is that from sources located external to the exposed individual, such as from gamma radiation from radionuclides deposited on the ground. Internal exposure results from inhalation of airborne radionuclides and ingestion of food contaminated with the pollutants. Internal exposure is dependent on the rate of radionuclide intake by inhalation and ingestion, uptake from the blood pool, buildup of the daughter radionuclides, and retention in the body.

Exposure pathways are broadly divided into internal and external routes (Fig. 1.2). External exposure results from the absorption of gamma and beta radiation emitted directly from tailings, ore and yellowcake product storage, contaminated soil, and airborne radioactivity. Internal exposure results from the inhalation of airborne radionuclides and the ingestion of food contaminated with radioactive substances. The rate of clearance from the lung is dependent on the transportability of the radionuclide, which is a function of particle size, intrinsic solubility in the lung, interstitial fluid of the lung, and interaction of the inhaled particles with local lung environment (see references at the end of this chapter).

The dose rate to any organ in the body from internal pathways is a function of the elapsed time since initiation of exposure and the spatial distribution of the radionuclides. In UDAD-IX the average organ dose rates are estimated because data on the local distributions of radionuclides at the cellular level as a function of time are not available. Dose--time integration of dose rate--is dependent on rate of uptake from the systemic blood pool, the

buildup of daughter radionuclides, and the retention of the radionuclides in tissue.

The following diagrams show the pattern of uptake as a result of a constant intake (I).
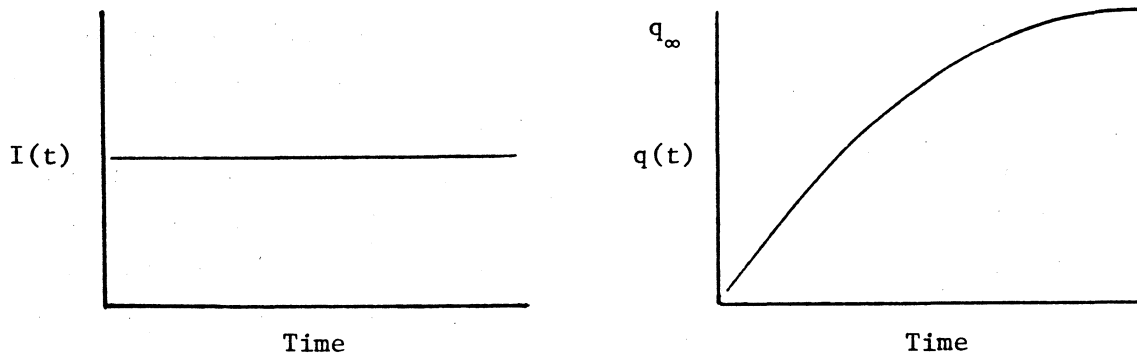
Chronic uptake at a constant rate of $I(t)$ will result in a body burden, $q(t)$, which will approach an equilibrium value, q_∞, after continuous intake (ICRP-6). However, for some nuclides in the ^{238}U series the duration of intake required to approach equilibrium is longer than human life expectancy. Uptake $[\frac{dq(t)}{dt}/I(t)]$ is age-dependent and is largest during skeletal ossification; i.e., in children and infants, for bone-seeking radionuclides. Uptake and retention for most radionuclides of interest are not known as a function of age. Hoenes and Soldat (1977) have estimated age-specific radiation dose commitments for several radionuclides.

For radiation workers, the maximum period of dose accumulation is about 50 years, but, for the general population, the exposure period can begin *in utero* and extend beyond the 70th year of age. The UDAD code calculates dose rate to reference man as a function of time over a period of 70 years.

Several radionuclides in the uranium-238 series (^{230}Th, ^{226}Ra) have both long physical half-lives and long biological retention periods relative to the human life span. For these radionuclides, the concentration of radioactivity in the tissues will increase with increasing duration of radioactivity intake

and will approach an equilibrium level assuming a constant rate of radio-activity intake. An interruption in the rate of intake, for example after decommissioning of the mill, will alter the ratio of uptake to intake values and will subsequently result in a decrease of the tissue concentration by relocation and excretion (Fig. 5.1). Within a 70-year life span the body burden of some radionuclides will not reach the state of radioactive equi-librium with the level of radioactivity intake—for example, thorium in bone. Also, the rate of uptake of the radioactivity in tissue, i.e., fraction of the radioactivity in the systemic blood incorporated in the tissue, may depend on one's physiological age. For example, radium uptake is a function of the rate of skeletal ossification and is higher from birth to maturity (about 20 years of age) than after skeletal maturity. Thus, the tissue concentration of radionuclides with long effective half-life will be dependent on the intake period and age during exposure. Age-dependence of radioactive uptake for humans is not known.

References for Section 5

Altshule, B., N. Nelson, and M. Kuschner, *Estimation of the Lung Dose from the Inhalation of Radon Daughters*, Health Physics, 10:1137, 1964.

Bair, W. J., et al., *Factors Affecting Retention, Translocation and Excretion of Radioactive Particles*, in "Radiological Health and Safety in Mining and Milling of Nuclear Material," IAEA Document STI/PUB/78, International Atomic Energy Agency, Austria, Vienna, 1964.

Chamberlain, A. C., and E. D. Dyson, *The Dose to the Trachi and Bronchi from the Decay Products of Radon and Thoron*, British Journal of Radiology, 29:137, 1956.

George, A. C., and L. Hinchliffe, *Measurement of Uncombined Radon Daughters in Uranium Mines*, Health Physics, V. 23, No. 6, 1972.

Hague, A. K. M. M., A. J. L. Collinson, "Radiation Dose to the Respiratory System due to Radon and Its Daughter Products," Health Physics, V. 13, p. 431, 1967.

Hatch, T. F., and P. Gross, *Pulmonary Deposition and Retention of Inhaled Aerosols*, Academic Press, New York, 1964.

Hoenes, G. R., and J. K. Soldat, *Age-Specific Radiation Commitment Factors for One-Year Chronic Intake*, Battelle Pacific Northwest Laboratory, November 1977.
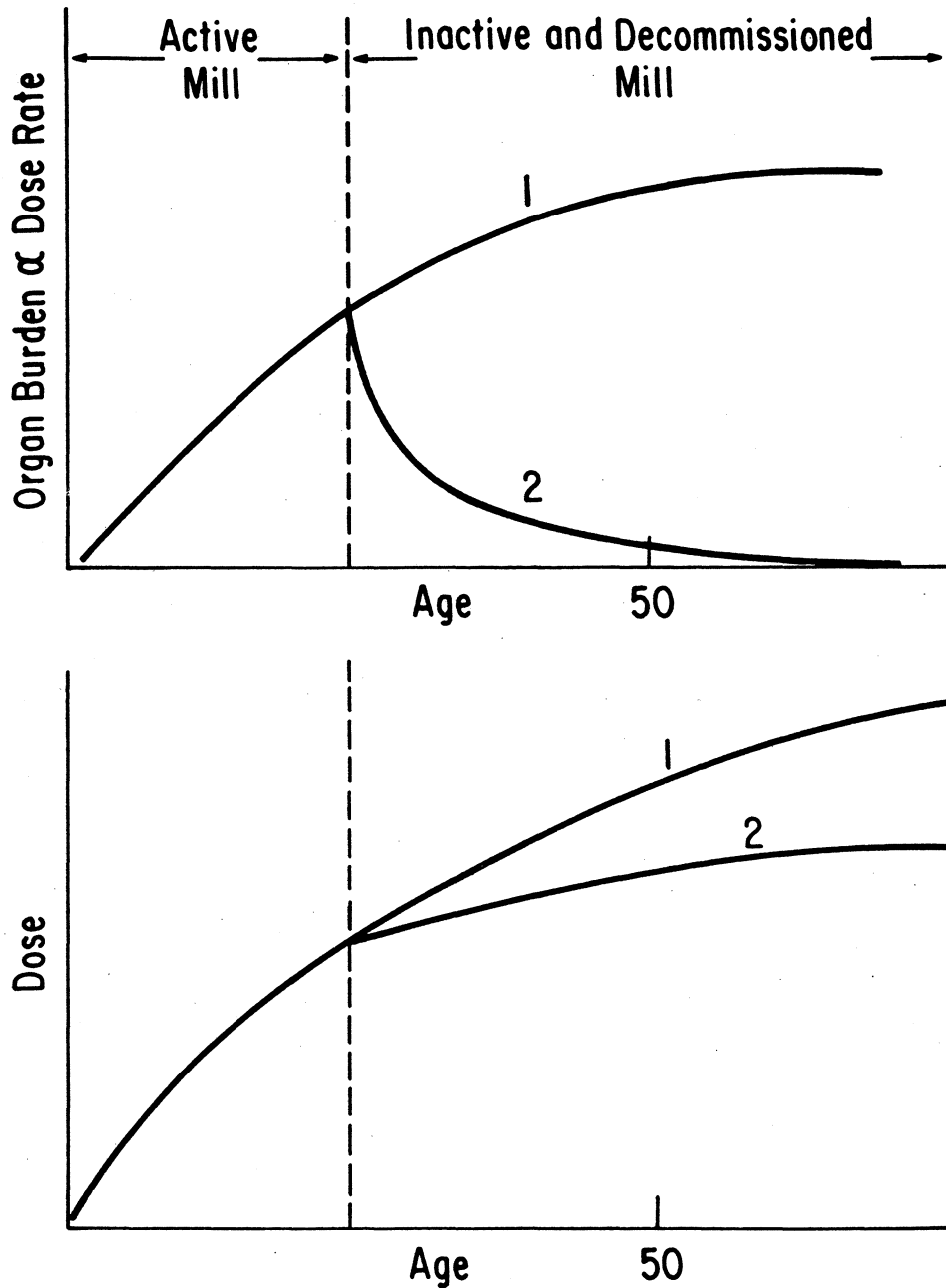
Fig. 5.1. Organ Burden as a Function of Duration (Age) of
Continuous Radionuclide Intake. The dose rate
at any age is proportional to the organ burden.
Curve 1 shows the dose rate and dose as a result
of continuous constant radionuclide intake from
birth through old age. Because of the limited
duration of mill operations, the concentration
of radionuclides in the intake will decrease
when mill operations cease, which results in
decreased dose and dose rates (Curve 2).

ICRP-II, Report of ICRP Committee II on Permissible Dose for Internal Radiation, Health Phys. 3:1-380, 1960.

ICRP-4, *Deposition and Retention Models for Internal Dosimetry of the Human Respiratory Tract*, Task Group on Lung Dynamics, Health Physics, 12:173, 1966.

ICRP-6, *Permissible Dose for Internal Radiation*, International Commission on Radiation Protection, Publication #6, Pergamon Press, 1964.

James, A. C., G. F. Bradford, D. M. Howell, *Collection of Unattached Ra Atoms Using a Wire Gauze*, Aerosol Science, V. 3, p. 243, 1972.

Lippman, M., and R. E. Albert, *The Effect of Particle Size on the Regional Deposition of Inhaled Aerosols in the Human Respiratory Tract*, American Industrial Hygiene Association Journal, V. 30, p. 257, 1969.

Morrow, P. E., Health Phys. 2:366-378, 1960.

Morrow, P. E., and L. J. Casarett, *An Experimental Study of the Deposition and Retention of a Plutonium-239 Dioxide Aerosol*, in "Inhaled Particles and Vapours," (Ed. C. N. Davies) Pergamon Press, N.Y., p. 167, 1961.

USAEC-18, *Models for the Study of Particle Retention and Elimination in the Lung*, in "Inhalation Carcinogenesis," U.S. Atomic Energy Commission Symposium Series #18, 1970.

6. EXTERNAL EXPOSURE

Sources of external exposure are the indirect radiation from airborne radionuclides and ground-deposited radioactive substances plus the direct gamma and beta emissions from ore on the ore pads and in the mill circuit and the tailing at the disposal sites. In UDAD, direct exposure is not treated.

6.1 EXTERNAL EXPOSURE FROM AIRBORNE AND GROUND-DEPOSITED ACTIVITIES

The dose rate $\dot{D}_{ec}(r,\theta,t;\Psi)$ to tissue Ψ (Fig. 1.2) from indirect external exposure to airborne radionuclides is given by:

$$\dot{D}_{ec}(r,\theta,t;\Psi) = \sum_i \delta(i)R_c(i,\Psi)<\chi(r,\theta,t;i)> , \qquad (6.1)$$

where $\delta(i)$ is the shielding factor for the radionuclide i from building structures,

$R_c(i,\psi)$ is the dose rate per unit concentration of i to the organ or tissue Ψ (dose rate factor), and

$<\chi(r,\theta,t;i)>$ is the total average airborne concentration of i at time t and location (r,θ).

In UDAD a constant shielding factor for the entire uranium-238 series was assumed even though the shielding factor is dependent on the gamma energy of each member of the series. The dose rate is calculated from:

$$\dot{D}_{ec}(r,\theta,t;\Psi) = \delta \sum_i R_c(i,\Psi)<\chi(r,\theta,t;i)> . \qquad (6.2)$$

Similarly, the dose rate $\dot{D}_{eg}(r,\theta,t;n)$ from ground-deposited radionuclides i is given by:

$$\dot{D}_{eg}(r,\theta,t;\Psi) = \sum_i \epsilon(i)R_g(i,\Psi)<\Gamma(r,\theta,t;i)> , \qquad (6.3)$$

where $\varepsilon(i)$ is the shielding factor for the radionuclide i,

$R_g(i,\Psi)$ is the dose rate per unit surface contamination, and

$<\Gamma(r,\theta,t;i)>$ is the total average surface contamination at location (r,θ) at time t by the radionuclide i. In UDAD, $\varepsilon(i) = \delta(i) =$ a constant, even though the shielding factor $\varepsilon(i)$ is not equivalent to R(i) because of dependence of the shielding factor on exposure geometry of the ground relative to the air.

The dose rate $\dot{D}_{eg}$ is calculated from:

$$\dot{D}_{eg}(r,\theta,t;\Psi) = \delta \sum_i R_g(i,\Psi)<\Gamma(r,\theta,t;i)> . \tag{6.4}$$

Tables 6.1 and 6.2 give, respectively, the dose rate factors for airborne and ground-deposited radionuclides. These dose rate factors include contributions from beta particles and are mainly adopted from Trubey and Kaye (1973) compilations. $R_c(i,\Psi)$ dose rate conversion factors were calculated from a semi-infinite space containing homogeneous radionuclide distribution. These dose rate factors may overestimate gamma dose components, as the atmospheric dispersion is not homogeneous in distribution of concentration in the vertical direction. The $R_g(i,\Psi)$ values were calculated for a height of one meter from an infinite ground plume containing a homogeneous surface contamination of the radionuclide i. Geometric attenuation factors for each organ were estimated using the Monto Carlo calculation method of Poston and Snyder (1974).

Dose, i.e,. the time-integrated dose rate, is calculated from:

$$D(r,\theta;\Psi) = \int_{t_o}^{t_e} \dot{D}(r,\theta,t;\Psi) \, dt + \int_{t_e}^{(t-t_e)} \dot{D}(r,\theta,t;\Psi) \, dt . \tag{6.5}$$

The dose to an individual is calculated for t_e, the duration of the active industrial operation, and for $(t - t_0)$ the period of occupancy at the site, where t_0 is the beginning year of industrial operation. The longest exposure period may correspond to a life-span exposure of 70 years ($\Delta t = t - t_0 = 70$ years). But in general, the exposed population is heterogeneous in age

Table 6.1. External Dose Rate Factors (mrem/year/pCi/m^3) for Airborne Radionculides [$R_c(i,\Psi)$]

Pollutant(i)	Skin	Whole Body	Ovaries	Testes	Small Intestine	Lung	Red Marrow	Skeleton	Spleen
U238	1.00E-04	1.57E-06	2.92E-07	1.29E-06	2.43E-07	4.77E-07	1.35E-06	1.53E-06	3.22E-07
TH234	6.22E-04	5.24E-05	2.28E-05	4.85E-05	3.25E-05	4.29E-05	8.60E-05	9.33E-05	3.12E-05
PA234	7.63E-03	1.22E-04	9.57E-05	8.06E-05	7.36E-05	8.94E-05	9.83E-05	1.08E-04	8.73E-05
U234	1.36E-04	2.49E-06	6.64E-07	2.09E-06	5.99E-07	1.03E-06	2.64E-06	2.94E-06	7.34E-07
TH230	1.46E-04	3.59E-06	1.52E-06	3.17E-06	1.33E-06	2.10E-06	4.83E-06	5.31E-06	1.67E-06
RA226	1.79E-04	4.90E-05	2.63E-05	6.27E-05	3.44E-05	4.33E-05	6.98E-05	7.52E-05	3.93E-05
RN222	3.46E-06	2.83E-06	1.04E-06	3.14E-06	2.05E-06	2.67E-06	3.30E-06	3.46E-06	2.99E-06
PO218	8.18E-07	6.34E-07	3.88E-07	5.72E-07	4.91E-07	5.93E-07	6.34E-07	6.95E-07	6.34E-07
PB214	4.89E-03	1.67E-03	7.46E-04	1.94E-03	1.17E-03	1.52E-03	2.15E-03	2.29E-03	1.57E-03
BI214	1.95E-02	1.16E-02	9.13E-03	9.29E-03	8.86E-03	1.10E-02	1.17E-02	1.26E-02	1.15E-02
PO214	9.89E-07	7.66E-07	4.70E-07	6.92E-07	5.93E-07	7.17E-07	7.66E-07	8.40E-07	7.66E-07
PB210	3.94E-04	1.43E-05	7.56E-06	1.21E-05	5.31E-06	9.05E-06	2.23E-05	2.45E-05	7.27E-06
BI210	3.56E-03	0.0	0.0	0.0	0.0	0.0	0.0	0.0	0.0

Table 6.2. External Dose Rate Factors (mrem/year/pci/m^2) for Ground-Deposited Radionuclides [$R_g(i,\Psi)$]

Pollutant(i)	Skin	Whole Body	Ovaries	Testes	Small Intestine	Lung	Red Marrow	Skeleton	Spleen
U238	2.13E-06	3.17E-07	5.89E-08	2.60E-07	4.90E-08	9.62E-08	2.73E-07	3.08E-07	6.49E-08
TH234	2.10E-06	1.66E-06	7.21E-07	1.53E-06	1.03E-06	1.36E-06	2.72E-06	2.96E-06	9.87E-07
PA234	1.50E-03	1.72E-06	1.17E-06	1.46E-06	1.32E-06	1.61E-06	1.77E-06	1.94E-06	1.58E-06
U234	2.60E-06	4.78E-07	1.27E-07	4.00E-07	1.15E-07	1.97E-07	5.05E-07	5.63E-07	1.40E-07
TH230	2.20E-06	6.12E-07	2.60E-07	5.40E-07	2.27E-07	3.59E-07	8.24E-07	9.06E-07	2.85E-07
RA226	1.16E-06	9.47E-07	5.07E-07	1.21E-06	6.63E-07	8.36E-07	1.35E-06	1.45E-06	7.58E-07
RN222	6.15E-08	5.03E-08	1.84E-08	5.59E-08	3.64E-08	4.76E-08	5.88E-08	6.15E-08	5.32E-08
PO218	1.42E-08	1.10E-08	6.73E-09	9.91E-09	8.50E-09	1.03E-08	1.10E-08	1.20E-08	1.10E-08
PB214	1.42E-04	3.16E-05	1.41E-05	3.66E-05	2.21E-05	2.88E-05	4.06E-05	4.32E-05	2.96E-05
BI214	1.20E-03	1.85E-04	1.47E-04	1.49E-04	1.42E-04	1.76E-04	1.88E-04	2.06E-04	1.85E-04
PO214	1.72E-08	1.33E-08	8.17E-09	1.20E-08	1.03E-08	1.25E-08	1.33E-08	1.46E-08	1.33E-08
PB210	6.65E-06	2.27E-06	1.20E-06	1.92E-06	8.45E-07	1.44E-06	3.56E-06	3.90E-06	1.16E-06
BI210	5.02E-04	0.0	0.0	0.0	0.0	0.0	0.0	0.0	0.0

38

distribution and migratory. Thus, if $D(r,\theta,\Delta t=70;\Psi)$ is used for estimation of radiological effects, the results will be overly conservative.

References for Section 6

Poston, J. W., and W. S. Snyder, *A Model for Exposure to a Semi-infinite Cloud of a Photon Emitter*, Health Physics, V. 26, No. 4, April 1974.

Trubey, D. K., and S. V. Kaye, *The EXREM V Computer Code for Estimating External Radiation Dose to Population from Environmental Releases*, Report ORNL-TM-4322, December 1973.

7. INGESTION

Ingestion of contaminated food is a pathway of exposure to the gastrointestinal tract and to other tissues by absorption into the systemic blood pool. Figure 7.1 schematically depicts the significant food pathways from direct contamination of food such as vegetables, water and grains and from indirect contamination of food such as meat. In both cases, the food is contaminated by ground deposition of airborne radionuclides and from the use of contaminated water. The effects of ground deposition are cumulative because of the low rate of depletion from the soil partially due to the small amount of precipitation (rain and snow). Because of the limited available data on the variables affecting radionuclide concentrations in food, only four major ingestion pathways are included in the present version of UDAD. These specific pathways are via vegetation, meat, milk and poultry and eggs.* For each region of food production, a centroid representing the average regional productivity is considered. The potential for food contamination by the effluents through ground deposition and water is computed. The regional food yield and the concentrations of the radionuclides for each centroid are utilized in the computation of the ingestion dose rate and dose and population exposure. Since water transport is not incorporated in this version of UDAD, dosimetry of water pathways is treated by introduction of nuclide concentrations (inputed) into the ingestion pathway.

---

*In earlier versions of UDAD, 21 food items were considered. But in this revision, the number was reduced because some items produced only relatively minor contributions to the ingestion pathway (e.g., fish--present mining and milling operations are not near large bodies of water) or could be combined (e.g., pork, mutton and beef). Vegetables were also grouped as above-ground (e.g., lettuce) and below-ground (e.g., potatoes) contributors. Like items were combined upon the recommendation of the USNRC.

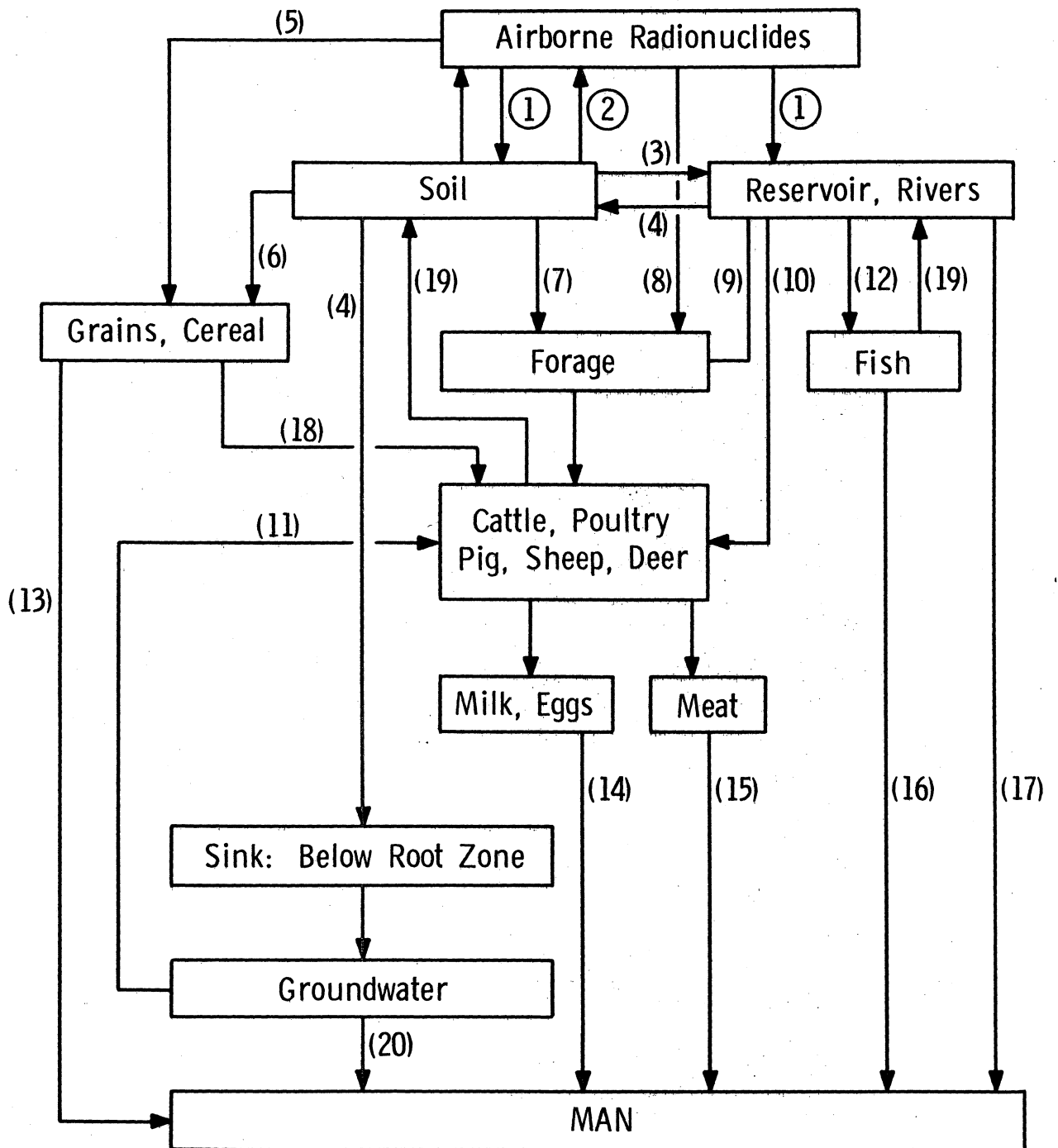# FOOD CHAINS LEADING TO MAN

Fig. 7.1. Food Chains Leading to Man. In this version of UDAD pathways leading from reservoirs, rivers, fish, and groundwater are not explicitly calculated.

41

7.1 RADIONUCLIDE CONCENTRATIONS IN VEGETATION AND PASTURES

The concentration of a radionuclide i in vegetation v or the pasture at a centroid (r,θ) from deposition on foliage and uptake from the prior contamination t in the soil is:

$$C(r,\theta,t;i,v) = 8.64 \times 10^4 \sum_{s} <\chi(r,\theta,t;i,s)>$$

$$V_d(s)\left\{\eta_v f_v[1 - \exp(\lambda_e(i)t_v)]/y_v\lambda_e(i)\right\} + \eta_v U_v(i)W(r,\theta,t;i)/\rho , \qquad (7.1)$$

where $V_d(s)$ is the deposition velocity from the total annual average airborne concentration χ for the effluents particles of size s,

η is the decontamination factor due to food processing, such as washing, peeling, etc., of the vegetation, but does not apply to forage, where $\eta = 1$.

f_v is the fraction of foliar deposition retained on the plant,

$\lambda_e(i) = \lambda(i) + \omega(i)$ is the effective removal constant of the radionuclide i from the plants, [$\lambda(i)$ is the radioactive decay coefficient and $\omega(i)$ is the weathering coefficient from the plant],

y_v is the yield factor (kg/m^2) per year,

t_v is the plant exposure period,

$U_v(i)$ is the plant uptake from the soil in pCi/kg of the plant per pCi/kg of the root zone soil,

ρ is the effective surface density of soil, and

$W(r,\theta,t;i)$ is the surface deposition concentration of radionuclide i throughout the time from start of deposition until harvest of the plant.

The default values for the Eq. 7.1 are:

$\eta = 0.5$ for vegetables consumed by man,

$\eta = 1.0$ for pasture and food crops consumed by the animals,

$$f_v = 0.2,$$

$$\omega(i) = 0.693/14 \text{ days},$$

$$y_v = 2.0 \text{ kg/m}^2 \text{ for crops},$$

$$y_v = 0.75 \text{ kg/m}^2 \text{ for pasture},$$

$$U_v(i) = \text{default values given in Table 7.1, and}$$

$$\rho = 240 \text{ kg/m}^2 \text{ assuming a uniform mixing of all radionuclides in a}$$
plowlayer of 15 cm depth.

However, the value for any of these parameters (default value) may be changed based on site-specific conditions and availability of new data.

Table 7.1. Default Parameters of Food Intake for Standard Man Utilized in UDAD[a,b]

Pathway	Average Exposed Individuals	Maximally Exposed Individuals
Vegetables, kg/day[b]	0.28	0.77
Meat, kg/day	0.26	0.30

[a] *These values are those for adults taken from Tables E-4 and E-5 of U.S. Nuclear Regulatory Commission Guide 1.109, Revision 1, October 1977.*

[b] *Does not include fruits or grain.*

Equation 7.1 can be applied to a variety of food crops, provided the appropriate parameters can be estimated. There is a wide range in the values for crop yield, time of exposure, factor for uptake from soil, translocation to edible parts of the plant, and effective surface density of soil. These parameters vary with the nuclide and the crop and depend heavily on location and soil properties. Since values of certain parameters could not be found in the literature for many of the nuclides of concern, in this model vegetation represents all vegetables and food crops. It is assumed that the concentration of radionuclides in the edible part of the plant is the same as the average concentration in overall plant.

7.2 RADIONUCLIDE CONCENTRATIONS IN MEAT, POULTRY, DAIRY AND EGGS

The radionuclide concentrations in meat (beef, mutton), poultry, dairy products and eggs are dependent on the animals total daily radionuclide intake from feeds (pastures, grains, stored feed), drinking water and inhalation. Inhalation rates for animals have been reported, but the transfer rates from inhalation for some of the radionuclides to the animal products are not known. Therefore, in this version of UDAD, contamination of the products from animal inhalation are not estimated. Based on the above consideration, the radio-nuclide concentrations in product k of the above animals, α, are expressed by:

$$C(r,\theta,t;i,\alpha(k)) = g(\alpha) \ F(i,\alpha(k)) \sum_{j} C_p(r,\theta,t;i,j)Q(\alpha,j) \ , \qquad (7.2)$$

where $C(r,\theta,t;i,\alpha(k))$ is the concentration of the radionuclide i in the product k of the animal α at centroid (r,θ) at time t,

$g(\alpha)$ is the fraction of the year animal α is on contaminated intake,

$F(i,\alpha(k))$ is the transfer coefficient of the radionuclide i to the product $\alpha(k)$,

$C_p(r,\theta,t;i,j)$ is the concentration of the radionuclide i from feed j at the centroid (r,θ), and

$Q(\alpha,j)$ is the consumption rate of the contaminated feed j by the animal α.

The default values adopted in this version of UDAD are:

$g(\alpha) = 0.5$ for all α

$F(i,\alpha(k))$ for meat/feed in days/kg are U (3.4×10^{-4}), Th (2.0×10^{-4}), Ra (4.0×10^{-3}), Pb (2.9×10^{-4}), and Po (1.2×10^{-2}).

$Q(\alpha,j) = 50$ kg/day for a pastured cow

$\quad\quad\quad = 0.12$ kg/day of grain for poultry.

The $C_p(r,\theta,t;i,j)$ is estimated from Eq. 7.1.

Because of lack of better input parameters, this version of UDAD assumes that cows consume only pasture grass and that poultry consumes only grain. The daily intake of the feed j is seasonally as well as climatically dependent on the site of the centroid. The transfer coefficient $F(i,\alpha(k))$ is the fraction of daily intake of the radionuclide i appearing in the product k of the animal α. Data reported on transfer coefficients are limited and not well documented. The transfer of radionuclides from air to plants through both leaves and soil and then to food products follows the methodology described in Regulatory Guide 1.109 except for Ra-226 (Scarano 1978).

7.3 INGESTION DOSIMETRY

The ingestion dose rate is estimated from the rate of radionuclide intake, rate of radioactive uptake, deposition, and the rate of clearance from each organ or tissue of interest, the rate of energy deposition in the organ and the organ weight. The rate of radioactivity intake is dependent on the daily food intake rate and the radionuclide concentrations in food. The radionuclide concentrations in foods are calculated based on the models described in the Sections 7.1 and 7.2. Since the radionuclides of concern in the ingestion pathway generally have long radioactive half-lives, loss and ingrowth in activity from radioactive decay during the time lag between production and consumption is not included.

The commonly used metabolic model and parameters for ingestion dose rate calculations are those presented in ICRP publication 2 (1959). The values utilized for metabolic pathways are selected from NRC report, Regulatory Guide 1.109 (1977). The ICRP model assumes that radioactivity retention in any organ follows a single-exponential function and is homogeneously distributed in the tissues. But recent experimental data seem to indicate multiple-exponential functions and a combination of exponential and power functions. The retention function is dependent on the age, health and metabolic state of the individual as well as the chemical form of the radionuclide. In UDAD, with the exception of computing dose rates to bone and whole body from ^{226}Ra, the metabolic models are those of ICRP 2 (1959). Dose rates for whole body and bone from radium-226 are calculated from a multiple-exponential retention model (ICRP-10A, 1971).

The burden, $Q(t;i,\Psi,j)$, of the radionuclide i in the organ or tissue Ψ from a continuous ingestion of the food type j at time t is given by:

$$\frac{dQ(t;i,\Psi,j)}{dt} = I(j)C(t,i,j)\ f_1(i)f_2'(i,\Psi) - \lambda(i,\Psi)Q(t;i,\Psi,j) ,\qquad (7.3)$$

where $I(j)$ is the rate of intake of food type j,

        $C(t;i,j)$ is the average concentration of radionuclide i in food j,

        $f_1(i)$ is the fraction of the radionuclide i that reaches the blood-stream from ingestion,

        $f_2^1(i,\Psi)$ is the fraction of $f_1(i)$ that reaches organ or tissue Ψ, and

        $\lambda(i,\Psi)$ is the effective decay constant of the organ Ψ, i.e., $\lambda(i,\Psi) = \lambda(i) + \lambda(\Psi)$ where $\lambda(i)$ and $\lambda(\Psi)$ are, respectively, the radioactive and biological coefficient for the radionuclide i and organ Ψ.

The biological half-lives $T_b(i,\Psi)$ and the radioactive half-lives $T_r(i)$ are, respectively, $\left(\dfrac{0.693}{\lambda(i,\Psi)}\right)$ and $\left(\dfrac{0.693}{\lambda(i)}\right)$.

The solution of Eq. 7.3 is:

$$Q(t;i,\Psi,j) = Q(0;i,\Psi,j)\ e^{-\lambda(i,\Psi)t} +$$

$$\frac{I(j)C(t;i,j)\ f(i)f_2'(i,\Psi)\left(1 - e^{-\lambda(i,\Psi)t}\right)}{\lambda(i,\Psi)} .\qquad (7.4)$$

The dose rate $\dot{D}$ in rem/day for the organ Ψ from the radionuclide i is:

$$\dot{D}(t;i,\Psi,j) = \frac{51.2 \times 10^{-6}\ Q(t;i,\Psi,j)E(i,\Psi)}{W(\Psi,t)} ,\qquad (7.5)$$

where Q is the body burden of i from j in the organ h in pCi,

        $E(i,\Psi)$ is the effective absorbed energy per disintegration for organ Ψ in $\dfrac{MeV \cdot rem}{dis \cdot rad}$, and

46

$W(\Psi, t)$ the weight of the organ h at time t in grams.

The time-integrated dose over the interval 0 - t, is given by:

$$D(t;i,\Psi,j) = \int_0^t \dot{D}(t;i,\Psi,j) \, dt \text{ (rem) }.$$ (7.6)

The solution of the Eq. 7.6 for an adult $[W(t,\Psi) = W(\Psi)]$ using the expression for organ or tissue burden and Eqs. 7.4 and 7.5 is:

$$D(t;i,\Psi,j) = \frac{51.2 \times 10^{-6} \, E(i,\Psi)}{\lambda(i,\Psi) \, W(\Psi)} \left\{ Q(0;i,\Psi,j) \left[\frac{1 - e^{-\lambda(i,\Psi)t}}{\lambda(i,\Psi)} \right] \right.$$

$$\left. + \frac{I(j)C(t,\Psi) \, f_1(i)f_2(i,\Psi)}{\lambda(i,\Psi)} \left(t - \left[\frac{1 - e^{-\lambda(i,\Psi)t}}{\lambda(i,\Psi)} \right] \right) \right\}.$$ (7.7)

The total dose rate and dose from all radionuclides and all types of food intake are given by:

$$\dot{D}(t;\Psi) = \sum_j \sum_i \dot{D}(t;i,\Psi,j)$$ (7.8)

and

$$D(t;\Psi) = \sum_j \sum_i D(t;i,\Psi,j) ,$$ (7.9)

from the Eqs. 7.5 and 7.7. For organs with subcompartments, such as bone with osteogenic and hematopoietic compartments, the total dose rate and dose are obtained by summations over compartments. The parameters used for the above equation are tabulated in Tables 7.1 and 7.2.

Table 7.2. Default Parameters of Internal Dose Rate Calculation

Nuclide (i)	Organ (Ψ)	$f_1(i)$	$f_2^1(i,h)$	T_r, days	T_b, days	$E(i)$ (QF), MeV rem/rad
U-238	WB	10^{-2}	1.0	1.6×10^{12}	100	43
	Bone	10^{-2}	0.11	1.6×10^{12}	300	220
	Liver	10^{-2}	0.0	1.6×10^{12}	–	–
	Kidney	10^{-2}	0.11	1.6×10^{12}	15	43
U-234	WB	10^{-2}	1.0	9.1×10^{7}	100	49
	Bone	10^{-2}	0.11	9.1×10^{7}	300	240
	Liver	10^{-2}	0.0	9.1×10^{7}	–	–
	Kidney	10^{-2}	0.11	9.1×10^{7}	15	49
Th-230	WB	10^{-4}	1.0	2.9×10^{7}	5.7×10^{4}	48
	Bone	10^{-4}	0.7	2.9×10^{7}	7.3×10^{4}	240
	Liver	10^{-4}	0.05	2.9×10^{7}	5.7×10^{4}	48
	Kidney	10^{-4}	0.05	2.9×10^{7}	2.2×10^{4}	48
Ra-226	WB & Bone	0.3	0.54	5.9×10^{5}	0.398	110
			0.29	5.9×10^{5}	4.95	
			0.11	5.9×10^{5}	57.75	
			0.04	5.9×10^{5}	6.93×10^{2}	
			0.02	5.9×10^{5}	5.33×10^{3}	
	Liver	0.3	0.0004	5.9×10^{5}	10	110
	Kidney	0.3	0.002	5.9×10^{5}	10	110
Pb-210	WB	0.08	1.0	7.1×10^{3}	1.46×10^{3}	5.2
	Bone	0.08	0.28	7.1×10^{3}	3.65×10^{3}	29
	Liver	0.08	0.08	7.1×10^{3}	1947	10
	Kidney	0.08	0.14	7.1×10^{3}	531	10
Po-210	WB	0.06	1.0	138.4	30	55
	Bone	0.06	0.1	138.4	24	280
	Liver	0.06	0.17	138.4	41	55
	Kidney	0.06	0.07	138.4	70	55

48

References for Section 7

Scarano, R. A., U.S. Nuclear Regulatory Commission, Value for radium taken from letter to P. F. Gustafson, Argonne National Laboratory, 25 July 1978 (see Appendix F).

ICRP-2, *Recommendations of the International Commission on Radiological Protection*, International Commission on Radiological Protection 2, Pergamon Press, London, 1959.

ICRP-10A, *Recommendations of the International Commission on Radiological Protection*, International Commission on Radiological Protection, Publication 10A, Pergamon Press, New York, 1971.

Regulatory Guide 1.109, *Calculation of Annual Doses to Man from Routine Releases of Reactor Effluents for the Purpose of Evaluating Compliance with 10 CFR Part 50, Appendix I*, U.S. Nuclear Regulatory Commission, Revision 1, October 1977.

New Regulatory Guide, *Age-Specific Radiation Dose Commitment Factors for One-Year Chronic Intake*, G. R. Hoenes, J. K. Soldat, Battelle Pacific Northwest Laboratories, November 1977.

8. INHALATION

*The dose and dose rate to the lungs and other organs from
inhalation of airborne radionuclides are dependent upon deposition
rate, chemical form, translocation and retention. Deposition of
airborne radionuclides on the epithelium of the respiratory system
occurs through the mechanisms of impaction, sedimentation and
diffusion. The fraction of the deposition is dependent on ana-
tomical structure, aerodynamic size distribution of the inhaled
aerosols and fraction of unattached ions on airborne particles
(Morrow and Cassarett 1961; Morrow 1960; Blair et al. 1964). The
dosimetry model in UDAD is based on the recommendations of the
Task Group on Lung Dynamics for Committee II of the International
Commission on Radiological Protection (1966).*

The human respiratory tract is divided into three major regions corre-
sponding to the sites of deposition of the radionuclides--the nasopharyngeal
(NP), the tracheobronchial (TB), and the pulmonary (P) regions. Figure 8.1
depicts the schematic structure of the respiratory model. A fraction of the
total activity inhaled is directly exhaled. The fraction of deposition of an
aerosol is dependent on the activity median aerodynamic diameter (AMD). The
deposition as a function of aerodynamic diameter for each region of the lung
is graphically reported in ICRP (1966).

Activity in each region is cleared from the blood pool for redistribution
and uptake by other tissues and organs (a,b,c). Further, a fraction of the
activity deposited in each of the regions is cleared into the gastrointestinal
tract (process b,d) for uptake by the blood pool (process j) and eventual
excretion. A fraction of the activity from pulmonary region is transported
into the lymph node system and cleared into the blood pool (i).

International Commission of Radiological Protection has classified
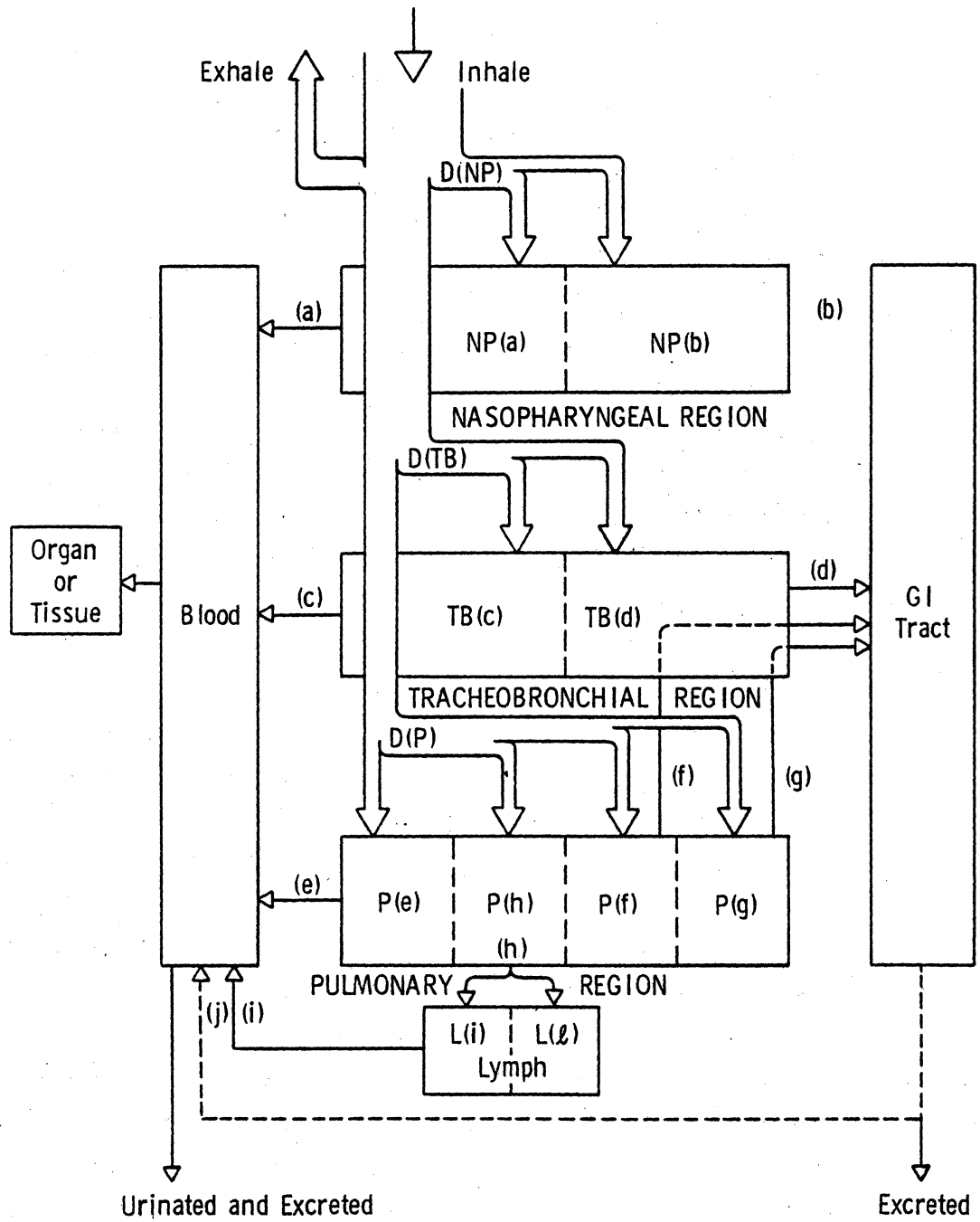inorganic compounds according to their relative rate of clearance from lung

Fig. 8.1. Schematic Diagram of the Task Group Lung Model
Used in UDAD.

into three transportability classes: Y, W, and D. The classes correspond to materials that clear slowly (in terms of years, Y), moderately (in weeks, W), or rapidly (in days, D). Solubility classification of uranium compounds released during product drying operations is not constant throughout the whole uranium milling industry. It is dependent on the nature of chemical extraction and drying temperature. It is assumed that uranium, thorium and polonium are in class Y, and that radium and lead are in class W. The values of the clearance rates for each clearance pathway are given in Table 8.1. Recent studies (Kalkwarf 1978) may suggest that the above classification should be modified; in UDAD the default solubility classifications are based on the recommendations of ICRP 1966 (task group lung dynamics).

8.1 RESPIRATORY TRACT RETENTION OF INHALED PARTICLES

The rate of deposition of radioactive particulates in the subcompartments ϕ of the Ψ compartment of the respiratory tract at time t is:

$$\frac{dQ(t;i,\Psi(\phi))}{dt} = \lambda^e(i,\phi) \; Q(t;i,\Psi(\phi)) + F(i,\Psi) \; f(i,\phi) \; , \tag{8.1}$$

$$F(i,\Psi) = I \sum_z D_z(\Psi) \; <\chi(r,\theta,\bar{t};z,i)> \; , \tag{8.2}$$

where $\lambda^e(i,\phi) = \lambda^b(i,\phi) + \lambda^r(i)$ is the effective removal constant of radionuclide i from the subcompartment ϕ. $\lambda^b(i,\phi)$ is the biological removal constant, and $\lambda^r(i)$ is the radioactive decay constant.

$Q(t;i,\Psi(\phi))$ is the burden of radionuclide i in the subcompartment ϕ of the Ψ compartment at time t,

$f(i,\phi)$ is the fraction removed from the ϕ subcompartment,

I is the air inhalation rate, and

$<\chi(r,\theta,\bar{t};i,z)>$ is the average concentration within a time interval of the radionuclide i in the air with aerodynamic diameter z, $z = s\sqrt{\rho}$. s and ρ are, respectively, activity median diameter and density, and

Table 8.1. Values of the Clearance Parameters, Biological Half-Life $T^b(i,\phi)$ (in days), and the Fraction Removed $f(i,\phi)$ for Each Translocation Class of Radionuclide i, from Subcompartment ϕ as Depicted in Figure 8.1 (Task Group Lung Model)

Respiratory Compartment	Metabolic Pathway	Translocation Class D		Translocation Class W		Translocation Class Y	
		$T^b(i,\phi)$	$f(i,\phi)$	$T^b(i,\phi)$	$f(i,\phi)$	$T^b(i,\phi)$	$f(i,\phi)$
NP:	a	0.01	0.5	0.01	0.1	0.01	0.01
	b	0.01	0.5	0.40	0.9	0.4	0.99
TB:	c	0.01	0.95	0.01	0.5	0.01	0.01
	d	0.2	0.05	0.2	0.5	0.2	0.99
P:	e	0.5	0.8	50.	0.15	500.	0.05
	f	–	–	1.	0.4	1.	0.4
	g	–	–	50.	0.4	500.	0.4
	h	0.5	0.2	50.	0.05	500.	0.15
L:	i	0.5	1.0	50.	1.	1000.	0.9

$D_z(\Psi)$ is the fraction of the inhaled particulate with aerodynamic diameter z deposited in the lung compartment Ψ.

The burden in $\Psi(\phi)$ from Eq. 8.1 is given by:

$$Q(t;i,\Psi(\phi)) = Q(0;i,\Psi(\phi)) \ A_{0,\phi}(t;i) +$$

$$F(i,\Psi) \ f(i,\phi) \ A_{1,\phi}(t;i) \ , \tag{8.3}$$

where

$$A_{0,\phi}(t;i) = \exp \ [-\lambda^e(i,\phi)t] \ , \tag{8.4}$$

and

$$A_{1,\phi}(t;i) = \frac{1 - \exp \ [-\lambda^e(i,\phi)t]}{\lambda^e(i,\phi)} \ . \tag{8.5}$$

For the NP and P compartments of the respiratory tract, the total tissue burden is the sum of the burdens resulting from deposition in the associated subcompartments in each. For the TB compartment, the burden is augmented by the processes f and g from the P compartment to the GI tract. The rate of change of the burden in the TB region as a result of these processes is:

$$\frac{dQ(t;i,TB(d))}{dt} = \sum_{\phi=f,g} \lambda^b(i,\phi) \ Q(t;i,P(\phi)) - \lambda^e(i,d) \ Q(t;i,TB(d)) \ . \tag{8.6}$$

The additional burden in the tracheobronchial region, calculated by integration of Eq. 8.6, is:

$$Q(t;i,TB(d)) = Q(0;i,TB(d)) \ A_{0,d}(t;i) +$$

$$\sum_{\phi=f,g} \lambda^b(i,\phi) \left\{ \frac{P(i,P) \ f(i,\phi)}{\lambda^e(i,\phi)} \left[A_{1,d}(t;i) - A_{\phi,d}(t;i) \right] + \right.$$

$$\left. Q(0;i,P(\phi)) \ A_{\phi,d}(t;i) \right\} \ , \tag{8.7}$$

where

$$A_{\phi_1,\phi_2}(t;i) = \frac{[\exp \ (-\lambda^e(i,\phi_1)t) - \exp \ (-\lambda^e(i,\phi_2)t)]}{\lambda^e(i,\phi_2) - \lambda^e(i,\phi_1)} \ . \tag{8.8}$$

The total tissue burden for the TB region is the sum of the tissue burdens as estimated by Eqs. 8.3 and 8.7.

The rate of change of pulmonary lymph node burden is:

$$\frac{dQ(t;i,L(i))}{dt} = \lambda^b(i,h)\ f(i,i)\ Q(t;i,P(h)) - \lambda^e(i,i)\ Q(t;i,L(i))\ . \qquad (8.9)$$

The lymph burden from Eq. 8.9 is:

$$Q(t;i,L(i)) = Q(0;i,L(i)\ A_{0,i}(t;i) +$$

$$\lambda^b(i,h)\ f(i,i) \left\{ \frac{F(i,P)\ f(i,h)}{\lambda^e(i,h)} \left[A_{1,i}(t;i) - A_{h,i}(t;i) \right] + \right.$$

$$\left. Q(0;i,P(h))\ A_{h,i}(t;i) \right\} \qquad (8.10)$$

for class Y solubility with $\lambda^e(i,h) \neq \lambda^e(i,i)$.

For classes W and D solubility with $\lambda^e(i,h) = \lambda^e(i,i)$, the lymph burden is:

$$Q(t;i,L(i)) = Q(0;i,L(i))\ A_{0,i}(t;i) +$$

$$\lambda^b(i,h)\ f(i,i) \left\{ \frac{F(i,P)\ f(i,h)}{\lambda^e(i,i)} \left[A_{1,i}(t;i) - A_{0,i}(i;i) \right] + \right.$$

$$\left. Q(0;i,P(h))\ t\ A_{0,i}(t;i) \right\} \ . \qquad (8.11)$$

For class Y solubility the additional material in $L(\ell)$ of the lymph nodes is:

$$Q(t;i,L(\ell)) = Q(0;i,L(\ell))\ A_{0,\ell}(t;i) + \lambda^b(i,h)(1 - f(i,i))$$

$$\left\{ \frac{F(i,P)\ f(i,h)}{\lambda^e(i,h)} \left[A_{1,\ell}(t;i) - A_{h,\ell}(t;i) \right] + \right.$$

$$\left. Q(0,i,P(h))\ A_{h,\ell}(t;i) \right\} \ . \qquad (8.12)$$

for $$\lambda^e(i,\ell) = \lambda^r(i) \ . \qquad (8.13)$$

The total burden in the lymph tissue is the sum of the two burdens estimated from Eqs. 8.10 or 8.11 and 8.12.

8.2 SYSTEMIC BLOOD ACTIVITY DISTRIBUTION TO ORGANS

The systemic blood pool is a common pathway for the distribution, accretion and reduction of radioactivity to and from organs. Organ burden is a result of the uptake and retention of radioactivity from the blood. In UDAD, the retention function from inhalation is assumed to be a single exponential function of time, except for ^{226}Ra in bone and whole body for which a multi-compartment exponential retention function is used.

Sources of blood activity and its distribution are schematically depicted in Figure 8.2. Based on this model the quantity of radioactivity that enters a given organ or tissue from the blood at any time t is assumed to be a constant fraction of the activity entering blood from the ingestion and inhalation pathways. ICRP II (1959) has designated this fraction f_2'. The rate of change of organ burden for the organ N or subcompartment n of the N is:

$$\frac{dQ(t;i,N(n))}{dt} = \sum_{\phi=a,c,e,i} \lambda^b(i,\phi) \ Q(t;i,\Psi(\phi)) \ f_2'(i,N(n)) \ +$$

$$\sum_{\phi=b,d,f,g} \lambda^b(i,\phi) \ Q(t;i,\Psi(\phi)) \ f_2'(i,N(n))f_1(i) \ -$$

$$\lambda^e(i,N(n)) \ Q(t;i,N(n)) \ , \qquad (8.14)$$

where f_1 is the fraction of the activity in the gut transported into the blood pool. Thus, the burden is:

$$Q(t;i,N(n)) = Q(0;i,N(n)) \ \dot{A}_{1,n}(t;i) \ +$$

$$\sum_{\phi=a,c,e} \lambda^b(i,\phi) \ f_2'(i,N(n)) \ B_{\phi,n}(t;i) \ +$$

$$\sum_{\phi=b,d,f,g} \lambda^b(i,\phi) \ f_2'(i,N(n)) \ f_1(i) \ B_{\phi,n}(t;i) + L_{N(n)}(t;i) \ , \qquad (8.15)$$
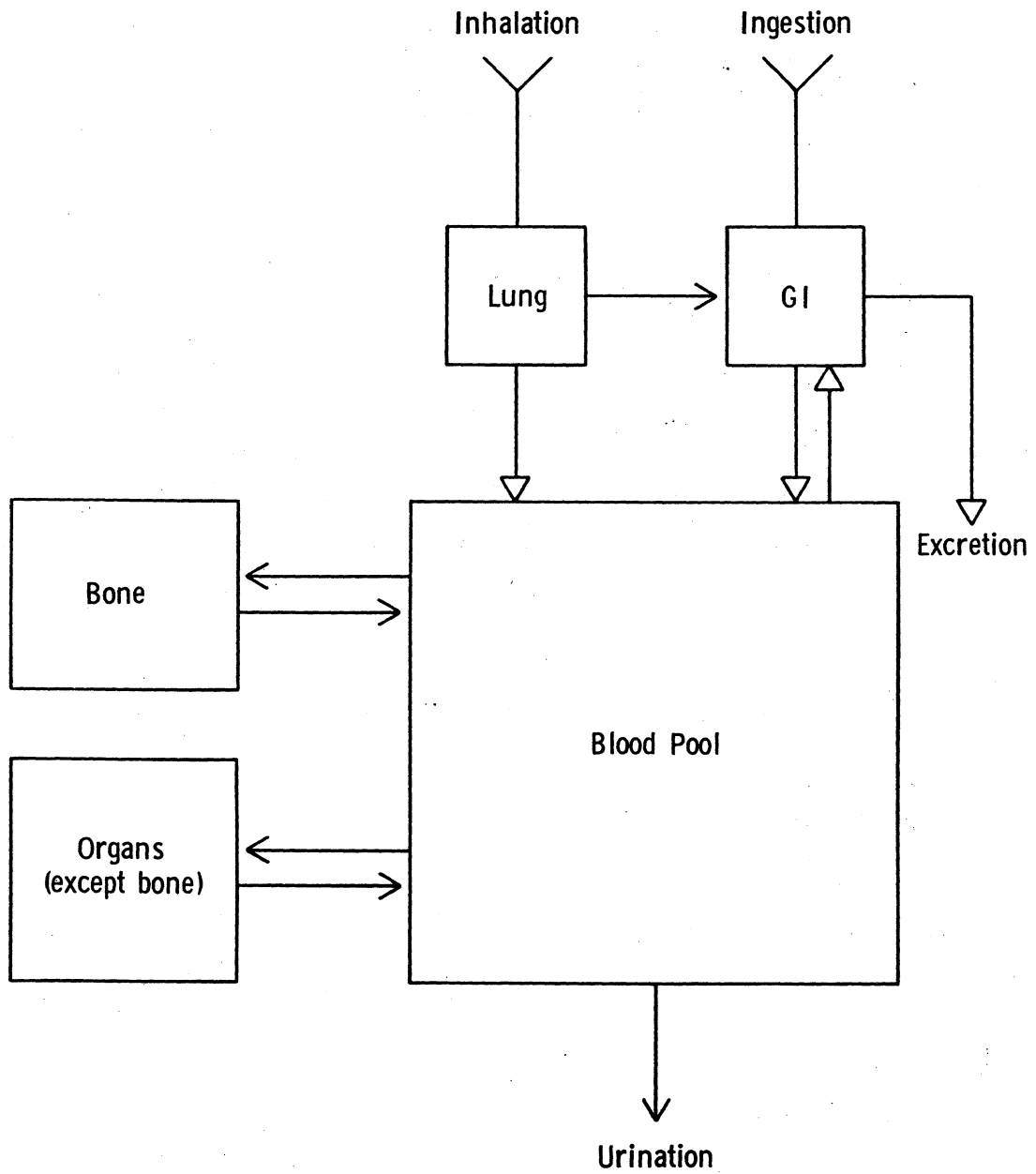
Fig. 8.2. Blood Pool System for Distributing
Radioactivity to Other Organs.

where

$$B_{\phi,n}(t;i) = \frac{F(i,\Psi(\phi))\ f(i,\phi)}{\lambda^e(i,z)} \left[A_{1,\phi}(t;i) - A_{\phi,n}(t;i) \right] +$$

$$Q(0;i,\Psi(\phi))\ A_{\phi,n}(t;i)\ . \tag{8.16}$$

$L_n(t;i)$ is the contribution to the organ burden from material passing through the lymphatic system.

For class Y solubility $\lambda^e(i,L(i)) \neq \lambda^e(i,h)$,

$$L_{N(n)}(t;i) = \lambda^b(i,i)\ f_2'(i,N(n))\ Q(0;i,L(i))\ A_{i,n}(t;i) +$$

$$\lambda^b(i,h)\ \lambda^b(i,i)\ f(i,i)\ f_2'(i,N(n)) \left\{ \frac{F(i,P)\ f(i,h)}{\lambda^e(i,h)} \right.$$

$$\left[\frac{A_{1,n}(t;i) - A_{i,n}(t;i)}{\lambda^e(i,i)} - \frac{A_{h,n}(t;i) - A_{i,n}(t;i)}{\lambda^e(i,i) - \lambda^e(i,h)} \right] +$$

$$\left. Q(0;i,P(h)) \left[\frac{A_{h,n}(t;i) - A_{i,n}(t;i)}{\lambda^e(i,i) - \lambda^e(i,h)} \right] \right\} . \tag{8.17}$$

For classes D and W solubility $\lambda^e(i,i) = \lambda^e(i,h)$,

$$L_{N(n)}(t;i) = \lambda^b(i,i)\ f_2'(i,N(n))\ Q(0;i,i)\ A_{i,n}(t;i) +$$

$$\lambda^b(i,h)\ \lambda^b(i,i)\ f(i,i)\ f_2'(i,N(n)) \left\{ \frac{F(i,p)\ f(i,h)}{\lambda^e(i,h)} \right.$$

$$\left[\frac{A_{1,n}(t;i) - A_{i,n}(t;i)}{\lambda^e(i,i)} - \frac{t\ A_{0,i}(t;i) - A_{i,n}(t;i)}{\lambda^e(i,n) - \lambda^e(i,i)} \right] +$$

$$\left. Q(0;i,P(h)) \left[\frac{t\ A_{0,i}(t;i) - A_{i,n}(t;i)}{\lambda^e(i,n) - \lambda^e(i,i)} \right] \right\} . \tag{8.18}$$

8.3 DOSE RATE AND DOSE

Dose rate to an organ or tissue is calculated from Eq. 7.5. The time-integrated doses are derived from Eqs. 7.5 and 7.6 using the organ or tissue burden given in previous subsections.

The dose to the NP region of the respiratory tract is:

$$D(t;i,NP) = \hat{D}(i,NP) \sum_{\phi=a,b} \left\{ \frac{F(i,NP)\ f(i,\phi)}{\lambda^e(i,\phi)} \right.$$

$$\left[t - A_{1,\phi}(t;i) \right] + Q(0;i,NP)\ A_{1,\phi}(t;i) \Bigg\} \tag{8.19}$$

for

$$\hat{D}(i,\Psi) = \frac{51.2 \times 10^{-6}\ E(i,\Psi)}{W(\Psi)} . \tag{8.20}$$

The dose to the TB region is:

$$D(t;i,TB) = \hat{D}(i,TB) \Bigg\{ \sum_{\phi=c,d} \left[\frac{F(i,TB)\ f(i,\phi)}{\lambda^e(i,\phi)} (t - A_{1,\phi}(t;i)) + \right.$$

$$Q(0;i,TB(\phi))\ A_{1,\phi}(t;i) \bigg] + Q(0;i,TB(d))\ A_{1,d}(t;i) +$$

$$\sum_{\phi=f,g} \left[\frac{\lambda^b(i,\phi)\ F(i,P)\ f(i,\phi)}{\lambda^e(i,\phi)} \left[\frac{t - A_{1,d}(t;i)}{\lambda^e(i,d)} - \frac{A_{1,\phi}(t;i) - A_{1,d}(t;i)}{\lambda^e(i,d) - \lambda^e(i,\phi)} \right] \right.$$

$$+ \lambda^b(i,\phi)\ Q(0;i,P(\phi)) \left[\frac{A_{1,\phi}(i;i) - A_{1,d}(t;i)}{\lambda^e(i,d) - \lambda^e(i,\phi)} \right] \bigg] \Bigg\} . \tag{8.21}$$

The dose to the P region is:

$$D(t;i,P) = \hat{D}(i,P) \sum_{\phi=e,f,g,h} \left\{ \frac{F(i,P)\ f(i,\phi)}{\lambda^e(i,\phi)} \left[t - A_{1,\phi}(t;i) \right] + \right.$$

$$Q(0;i,P(\phi))\ A_{1,\phi}(t;i) \Bigg\} \tag{8.22}$$

The dose to the lymph nodes is:

$$D(t;i,L) = \hat{D}(i,L) \left\{ Q(0;i,L(i))\, A_{1,i}(t;i) + \right.$$

$$\lambda^b(i,h)\, f(i,i) \left[\frac{F(i,P)\, f(i,h)}{\lambda^e(i,h)} \left(\frac{t - A_{1,i}(t;i)}{\lambda^e(i,i)} - \frac{A_{1,h}(t;i) - A_{1,i}(t;i)}{\lambda^e(i,i) - \lambda^e(i,h)} \right) \right.$$

$$\left. + Q(0;i,P(h)) \left(\frac{A_{1,h}(t;i) - A_{1,i}(t;i)}{\lambda^e(i,i) - \lambda^e(i,h)} \right) \right] + Q(0,i,L(\ell))\, A_{1,\ell}(t;i)$$

$$+ \lambda^b(i,h)\, (1 - f(i,i)) \left[\frac{F(i,P)\, f(i,h)}{\lambda^e(i,h)} \left(\frac{t - A_{1,\ell}(t;i)}{\lambda^r(i)} - \right. \right.$$

$$\frac{A_{1,h}(t;i) - A_{1,\ell}(t;i)}{\lambda^r(i) - \lambda^e(i,h)} \right) +$$

$$\left. \left. Q(0;i,P(h)) \left(\frac{A_{1,h}(t;i) - A_{1,\ell}(t;i)}{\lambda^r(i) - \lambda^e(i,h)} \right) \right] \right\}, \qquad (8.23)$$

for solubility class Y, and

$$D(t;i,TB) = \hat{D}(i,TB) \left\{ Q(0;i,L(i))\, A_{1,i}(t;i) + \right.$$

$$\lambda^b(i,h)\, f(i,i) \left[\frac{F(i,P)\, f(i,h)}{\lambda^e(i,h)} \left(\frac{t(1 + A_{0,i}(t;i)) - 2A_{1,i}(t;i)}{\lambda^e(i,i)} \right) - \right.$$

$$\left. \left. Q(0;i,h) \left(\frac{t\, A_{0,i}(t;i) - A_{1,i}(t;i)}{\lambda^e(i,i)} \right) \right] \right\} \qquad (8.24)$$

for solubility classes D and W.

For other organs and tissues, except for the GI tract, the time-integrated dose is:

$$D(t;i,N(n)) = \hat{D}(i,N) \left\{ Q(0;i,N(n)) \, A_{1,n}(t;i) + \right.$$

$$\sum_{\phi=a,c,e} \lambda^b(i,\phi) \, f_2'(i,N(n)) \, \mathcal{B}_{\phi,n}(t;i) +$$

$$\left. \sum_{\phi=b,d,f,g} \lambda^b(i,\phi) \, f_2'(i,N(n)) \, f_1(i) \, \mathcal{B}_{\phi,n}(t;i) + L_n(t;i) \right\}, \qquad (8.25)$$

where

$$\mathcal{B}_{\phi,n}(t;i) = \frac{F(i,\Psi(\phi)) \, f(i,\phi)}{\lambda^e(i,\phi)} \left[\frac{t - A_{1,n}(t;i)}{\lambda^e(i,n)} - \right.$$

$$\left. \frac{A_{1,\phi}(t;i) - A_{1,n}(t;i)}{\lambda^e(i,n) - \lambda^e(i,\phi)} \right] + Q(0;i,\Psi(\phi)) \left[\frac{A_{1,\phi}(t;i) - A_{1,n}(t;i)}{\lambda^e(i,n) - \lambda^e(i,\phi)} \right] \quad (8.26)$$

and

$$L_n(t;i) = \lambda^b(i,i) \, f_2'(i,N(n)) \left\{ Q(0;i,L(i)) \left[\frac{A_{1,i}(t;i) - A_{1,n}(t;i)}{\lambda^e(i,n) - \lambda^e(i,i)} \right] + \right.$$

$$\lambda^b(i,h) \, f(i,i) \left[\frac{F(i,P) \, f(i,h)}{\lambda^e(i,h)} \left[\frac{1}{\lambda^e(i,i)} \left(\frac{t - A_{1,n}(t;i)}{\lambda^e(i,n)} - \frac{A_{1,i}(t,i) - A_{1,n}(t;i)}{\lambda^e(i,n) - \lambda^e(i,i)} \right) \right. \right.$$

$$- \frac{1}{\lambda^e(i,i) - \lambda^e(i,h)} \left(\frac{A_{1,h}(t;i) - A_{1,n}(t;i)}{\lambda^e(i,n) - \lambda^e(i,h)} - \frac{A_{1,i}(t;i) - A_{1,n}(t;i)}{\lambda^e(i,n) - \lambda^e(i,i)} \right) \right]$$

$$\left. \left. + \frac{Q(0;i,h)}{\lambda^e(i,i) - \lambda^e(i,h)} \left(\frac{A_{1,h}(t;i) - A_{1,n}(t;i)}{\lambda^e(i,n) - \lambda^e(i,h)} - \frac{A_{1,i}(t;i) - A_{1,n}(t;i)}{\lambda^e(i,n) - \lambda^e(i,i)} \right) \right] \right\}$$

$$(8.27)$$

for class Y solubility, and

$$L_n(t;i) = \lambda^b(i,i)\ f_2'(i,N(n)) \left\{ Q(0;i,L(i)) \left[\frac{A_{1,i}(t;i) - A_{1,n}(t;i)}{\lambda^e(i,n) - \lambda^e(i,i)} \right] + \right.$$

$$\lambda^b(i,h)\ f(i,i) \left[\frac{F(i,P)\ f(i,h)}{\lambda^e(i,h)} \left[\frac{1}{\lambda^e(i,i)} \left(\frac{t - A_{1,n}(t;i)}{\lambda^e(i,n)} - \frac{A_{1,i}(t,i) - A_{1,n}(t;i)}{\lambda^e(i,n) - \lambda^e(i,i)} \right) \right. \right.$$

$$\left. - \frac{1}{\lambda^e(i,n) - \lambda^e(i,i)} \left(\frac{A_{1,i}(t;i) - t\ A_{0,i}(t;i)}{\lambda^e(i,i)} - \frac{A_{1,i}(t;i) - A_{1,n}(t;i)}{\lambda^e(i,n) - \lambda^e(i,i)} \right) \right]$$

$$\left. \left. + \frac{Q(0;i,h)}{\lambda^e(i,n) - \lambda^e(i,i)} \left(\frac{A_{1,i}(t;i) - t\ A_{0,i}(t;i)}{\lambda^e(i,i)} - \frac{A_{1,i}(t;i) - A_{1,n}(t;i)}{\lambda^e(i,n) - \lambda^e(i,i)} \right) \right] \right\}$$

(8.28)

for classes D and W solubility.

The basis for dosimetry of the gastrointestinal tract is ICRP II (1959) and the references therein. The dose rate to each part of the gastrointestinal tract (stomach, small intestine, upper larger intestine, and lower large intestine) is a function of the radionuclide residence period and the quantity absorbed from the gut into the blood pool. In the ICRP II (1959) model of the gastrointestinal tract only absorption of radionuclides in the small intestine is considered.

The rate of radionuclides reaching the GI tract from the respiratory system is:

$$\frac{dQ(t;i,GI)}{dt} = \sum_{\phi=b,d,f,g} \lambda^b(i,\phi)\ Q(t;i,\phi)$$

(8.29)

The total amount entering the gastrointestinal tract, calculated by integration of Eq. 8.29 is:

$$Q(t;i,GI) = \sum_{\phi=b,d,f,g} \lambda^b(i,\phi) \left\{ \frac{F(i,\Psi(\phi))\ f(i,\phi)}{\lambda^e(i,\phi)} \right.$$

$$\left. \left[t - A_{1,\phi}(t;i) \right] + Q(0;i,\phi)\ A_{1,\phi}(t;i) \right\}.$$

(8.30)

The dose $D(t;i,GI(s))$ to the stomach from the inhaled radionuclide i appearing in the gastrointestinal tract is:

$$D(t;i,GI(s)) = \hat{D}(i,s)Q(t;i,GI)\left[\frac{1 - e^{-\lambda_r(i)\tau_s}}{\lambda_r(i)}\right], \qquad (8.31)$$

where $\hat{D}(i,s)$ is the dose conversion factor, and

τ_s is the mean residence time of the radionuclide in the stomach.

The dose conversion factors calculated from Eq. 8.20 are reduced by one-half for all compartments of the GI tract because of geometric consideration.

The absorption of the radionuclide in the small intestine is assumed to be constant at a rate of λ_{f_1}:

$$\lambda_{f_1} = \frac{1}{\tau_{SI}} \ln\left[\frac{1}{1 - f_1}\right], \qquad (8.32)$$

where f_1 is the fraction of the radioactivity absorbed into the blood pool, and

τ_{SI} is the mean residence period in the small intestine.

In UDAD τ_{SI} is assumed to be four hours. The dose to the small intestine $D_{SI}(t;i)$ is:

$$D(t;i,GI(SI)) = \hat{D}(i,SI) \, Q(t;i,GI) \, \exp(-\lambda^r(i)\tau_s)\left[\frac{1 - \exp(-\lambda^e(i,SI)\tau_{SI})}{\lambda^e(i,SI)}\right]$$

$$(8.33)$$

where

$$\lambda^e(i,SI) = \lambda^r(i) + \lambda_{f_1} . \qquad (8.34)$$

The passage rate of material through the upper large intestine is assumed to be constant with a mean residence time τ_{ULI} of eight hours. The dose to the upper large intestine is:

$$D(t;i,GI(ULI)) = \hat{D}(i,ULI) \; Q(t;i,GI) \; (1 - f_1)\tau_{ULI} \; \exp \; (-\lambda^r(i)(\tau_s + \tau_{SI}))$$

$$(8.35)$$

The dose to the lower large intestine (LLI) is similar to that of the ULI except for the radioactive decay during passage through the ULI:

$$D(t;i,GI(LLI)) = \hat{D}(i,LLI) \; Q(t;i,GI) \; (1 - f_1)\tau_{LLI} \; \exp \; (-\lambda^r(i)(\tau_s + \tau_{SI} + \tau_{ULI}))$$

$$(8.36)$$

where τ_{LLI} is the mean residence time of 18 hours in the LLI.

8.4 RADON DOSIMETRY

The radiation dose from inhalation of radon and its daughters depends on their emitted alpha energies and radioactivities, on the body tissues they are retained in, and the period of time retained there. Earlier investigation have indicated that the radiation dose to the respiratory tract by inhalation of ^{222}Rn, a noble gas, is negligibly small compared with dose which results from the inhalation of the short-lived, non-gaseous decay products. The short-lived radon daughters ^{218}Po and ^{214}Po emit with 6.0 and 7.68 MeV energies, respectively. These nuclides emit alpha particles and are inhaled as ion or aerosol particles. They are deposited on the mucus layer covering the respiratory system. The radiation dose from the inhalation of radon and its daughters is dependent on the degree of equilibrium between radon and its daughters, and the physical state and sizes of the inhaled radioactive particles at the time of exposure.

The degree of equilibrium between radon and daughters in the atmosphere is a function of distance from the radon emanating source and the mean wind speed (Eq. 3.2). Inside a structure, the equilibrium condition is dependent on the air ventilation rate and the hold-up time. Attachment of the ions of radon daughters on the atmospheric aerosols is dependent on the atmospheric concentration of the airborne particles. These radon daughters behave as particulates during inhalation and deposition in the respiratory system. A review of problems of lung dosimetry of radon has been reported by Parker (1969).

In the present version of UDAD, the calculation of the radiation dose from inhalation of radon and its daughters is calculated for the bronchial epithelium of the tracheobronchial (TB) region. For indoor exposure, every 100 pCi/liter of Rn-222 present in air is assumed to be associated with 0.5 working level (WL) of short-lived radon daughters (Magno, 1978). For exposure to radon daughters outdoors the working level is calculated by Eq. 3.3. The radiation dose from inhalation is dependent on the breathing rate and the exposure duration. The exposure unit previously applied to the uranium miners is the working level month (WLM), i.e., the product of WL and the duration of exposure, normalized to a 172-hour working month exposure. But for the general population the exposure is continuous and the breathing rate is lower and shallower. In UDAD, for a continuous exposure to 1 WL for a year, a default value of 25 WLM is assumed (Magno, 1978). Conversion of WLM to a dose-equivalent of 5 rem/WLM is based on data provided by the committee on the Biological Effects of Ionizing Radiation (BEIR 1972). Under these conditions the annual average radiation dose rate to the bronchial epithelium of an individual is:

$$\dot{D}(r,\theta,t;Rn) = 0.625\ f_I <\chi(r,\theta,t;Rn)>$$

$$+\ 1.25 \times 10^5\ (1 - f_I)WL_0(r,\theta,t)\ , \tag{8.37}$$

where $\dot{D}(r,\theta,t;Rn)$ is the dose rate from radon daughters in mrem/year,

f_I is the frequency of occupancy indoors,

0.625 is the conversion factor in mrem per pCi/m^3,

1.25×10^5 is the conversion factor in mrem/WL, and

$WL_0 (r,\theta,t)$ is the outdoor working level.

References for Section 8

BEIR Report, *Biological Effects on Populations of Exposure to Low Levels of Radiation*, Division of Medical Sciences, National Academy of Sciences, Washington, D.C., 1972.

Blair, W. J., et al., *Factors Affecting Retention, Translocation and Excretion of Radioactive Particles*, in "Radiological Health and Safety in Mining and Milling of Nuclear Material," IAEA Document STI/PUB/78, International Atomic Energy Agency, Austria, Vienna, 1964.

ICRP, *Deposition and Retention Models for Internal Dosimetry of the Human Respiratory Tract*, International Commission on Radiological Protection, Task Group on Lung Dynamics, Health Physics, 12:173-207, 1966.

ICRP-II, Report of ICRP Committee II on Permissible Dose for Internal Radiation, 1959. See Health Phys. 3:1-380, 1960.

Kalkwarf, D. R., *Solubility Classification of Airborne Products from Uranium Ores and Tailings Piles*, Battelle Pacific Northwest Laboratory report, November 1978.

Magno, P. J. Memo to M. Momeni, March 10, 1978, *See Appendix F.*

Morrow, P. E., Health Phys. 2:366-378, 1960.

Morrow, P. E., and L. J. Casarett, *An Experimental Study of the Deposition and Retention of a Plutonium-239 Dioxide Aerosol*, in "Inhaled Particles and Vapours" (Ed. C. N. Davies), Pergamon Press, N.Y., p. 167, 1961.

Parker, M. H., *The Dilemma of the Lung Dosimetry*, Health Physics 16:553-561, 1969.

9. POPULATION DOSE COMMITMENT

Population dose commitments from inhalation, ingestion and external exposure are calculated for the population within an 80-km radius of the release site. The 80-km region is divided into a number of subregions (sector-segments) according to the population distribution. The subregion population for the last year of operation is estimated from regional demography and is introduced as input data.

The population dose commitment is calculated from the average radionuclide concentration and the exposure rate for each subregion. The total population dose commitment $D^P(t;\Psi,k)$ is:

$$D^P(t;\Psi,k) = \sum_d \sum_i P_d(t)\hat{D}_{i\Psi k}C_{ik}(t;d) , \tag{9.1}$$

where $P_d(t)$ is the population at time t within the subregion d,

$\hat{D}_{i\Psi k}$ is the individual dose commitment conversion factor to organ Ψ from the radionuclide i in pathway k, and

$C_{ik}(t;d)$ is the average concentration of the radionuclide i in the subregion d and pathway k.

The total population dose commitment from the ingestion pathway is calculated from the average radionuclide concentration in food. The radio-activity concentrations in foods that are produced within the 80-km radius are weighted and then averaged over the entire region. The weight factors are calculated from the concentrations in each food for each centroid by a food-utilization factor. This weight-average concentration of radionuclide i in food β is calculated by:

$$<C_{i\beta}(t)> = \sum_\zeta C_{i\beta}(t;\zeta)U_{\zeta\beta} , \tag{9.2}$$

where $U_{\zeta\beta}$ is the ratio of contribution of food β from centroid ζ to the population within the 80-km radius to the total consumption of food β within the 80-km radius,

$<C_{i\beta}(t)>$ is 80-km average concentration of nuclide i in food β, and

$C_{i\beta}(t,\zeta)$ is the concentration of radionuclide i in food β produced from centroid ζ.

The total population dose commitment from the ingestion pathway is then:

$$D^P(t;\Psi) = P(t) \sum_\beta \sum_i \hat{D}_{i\Psi} I_\beta <C_{i\beta}(t)> , \qquad (9.3)$$

where $P(t)$ is the total population within the 80-km radius of the site at time t,

$\hat{D}_{i\Psi}$ is the dose commitment conversion factor for ingestion of radionuclide i for organ or tissue Ψ, a factor that converts the intake rate of radionuclide i to the radiation dose commitment to organ or tissue Ψ, and

I_β is the intake rate of food β for an average individual.

The dose commitment factor is a 50-year time integrated dose rate resulting from only one year of chronic uniform ingestion of one pCi per day. The default values of intake rates for average exposed individual are given in Table 11.3.

10. ENVIRONMENTAL DOSE COMMITMENT

Contamination of the environment by long-lived radionuclides
represents a long-term potential source of exposure to humans.
The total radiological impact to a population following a given
release is dependent on the sum of all doses to individuals over
the entire time period the material persists in the environment
in a state available for interaction with humans.

The environmental dose commitment is calculated in UDAD for the population within an 80-km radius of the release site. The environmental dose commitment for an organ or a tissue Ψ resulting from exposure to radionuclide i via pathway k is:

$$D^e_{i,\Psi,k} = \sum_\zeta \int_0^{t_f} P(\zeta,t) D^a_{i,\Psi,k}(\zeta,t) \, dt \; , \tag{10.1}$$

where $D^e_{i,\Psi,k}$ is the environmental dose commitment for organ Ψ, radionuclide
i, pathway k for population exposure period t_f,

$P(\zeta,t)$ is the population associated with subregion ζ at time t, and

$D^a_{i,\Psi,k}(\zeta,t)$ is the average individual dose commitment for organ Ψ
from radionuclide i via pathway k and subregion ζ, and time t.

The calculation of environmental dose commitments by Eq. 10.1 requires a population projection for each subregion. Since long-range estimation of a detailed population projection is difficult and somewhat impractical. In UDAD an average regional population growth rate is assumed and applied to all subregions. Thus, the population projection for a subregion is given by:

$$P(\zeta,t) = G(t)P(\zeta,t=0) \; , \tag{10.2}$$

where G(t) is the function representing the average population growth rate in the subregion ζ, given by:

$$G(t) = \sum_\zeta P(\zeta,t) / \sum_\zeta P(\zeta,t=0) \; . \tag{10.3}$$

The average individual dose commitment to organ Ψ from an exposure pathway k in terms of concentration is:

$$D^a_{i,\Psi,k}(\zeta,t) = \hat{D}_{i,\Psi,k} C^a_{ik}(\zeta,t) ,$$ (10.4)

where $C^a_{ik}(\zeta,t)$ is the average concentration of radionuclide i via pathway k at subregion ζ and time t, and

$\hat{D}_{i,\Psi,k}$ is the individual dose commitment conversion factor for organ Ψ, radionuclide i, and pathway k.

Substitution of the Eqs. 10.2 and 10.4 into Eq. 10.1 results in:

$$D^e_{i,\Psi,k} = \sum_{\zeta} \underline{P}(\zeta,t=0)\hat{D}_{i,\Psi,k} \int_{t_1}^{t_f} G(t)C^a_{i,k}(\zeta,t) \, dt .$$ (10.5)

Expression 10.5 is integrated over m fixed time steps. For each time step Δt the average population growth is estimated for the midpoint of the time interval by:

$$D^e_{i,\Psi,k} = \sum_{\zeta} P(\zeta,t=0) \sum_{\delta=1}^{m} G(\bar{t}_\delta)\hat{D}_{i,\Psi,k} \int_{t_\delta}^{t_{\delta+1}} C^a_{i,k}(\zeta,t) \, dt ,$$ (10.6)

where
$$\bar{t}_\delta = \frac{t_{\delta+1} + t_\delta}{2}$$ (10.7)

Total environmental dose commitment to organ Ψ from pathway k is obtained by summing the contribution from each radionuclide i:

$$D^e_{\Psi,k} = \sum_{i} D^e_{i,\Psi,k} .$$ (10.8)

The following equations are derived from Eq. 10.8 by integration of the radionuclide concentration for each time interval.

10.1 ENVIRONMENTAL DOSE COMMITMENT FROM INHALATION OF PARTICULATES

The inhalation pathway is designated by k = 1 (see Section 4).

$$D^e_{i,\Psi,k} = \sum_{\zeta} P(\zeta,t=0) \sum_{\delta=1}^{4} G(\bar{t}_\delta) \sum_{s=1} \hat{D}_{i,\Psi,1}(s)I_{1,\delta}(\zeta,s) ,$$ (10.9)

69

where $I_{i,\delta}(\zeta,s)$ is defined as:

$$I_{i,\delta}(\zeta,s) = \int_{t_\delta}^{t_{\delta+1}} [<\chi(\zeta;s,i)> + <\chi^R(\zeta,t;s,i)>]\, dt \ . \tag{10.10}$$

For $\delta = 1$

$$I_{i,1}(\zeta,s) = t_a<\chi(\zeta;s,i)> + \sum_{h=1}^{i}\Bigg\{ k(0)<\chi(\zeta;s,h)>$$

$$V_d(s,h)\left(\prod_{\ell=h+1}^{i}\lambda_\ell\right)\sum_{\ell=h}^{i}\left[\frac{t_a\beta_\ell - \left(1 - e^{-\beta_\ell t}\right)}{\beta_\ell^2 \prod_{\substack{f=h\\f\neq\ell}}^{i}(\lambda_f - \lambda_\ell)}\right]\Bigg\} \ . \tag{10.11}$$

For $\delta = 2$

$$I_{i,2}(\zeta,s) = (t_e - t_a)<\chi(\zeta;s,i)> + \sum_{h=1}^{i}\Bigg\{ k(0)<\chi(\zeta;s,h)>$$

$$V_d(s,h)\left(\prod_{\ell=h+1}^{i}\lambda_\ell\right)\sum_{\ell=h}^{i}\left[\frac{(t_e - t_a)\left(1 - e^{\beta_\ell t_a}\right)}{\beta_\ell \prod_{\substack{f=h\\f\neq\ell}}^{i}(\lambda_f - \lambda_\ell)}\right]\Bigg\} +$$

$$\sum_{h=1}^{i}\Bigg\{ K_f<\chi(\zeta;s,h)V_d(s,h)\left[\prod_{\ell=h+1}^{i}\lambda_\ell\right]$$

$$\sum_{\ell=h}^{i}\left[\frac{(t_e - t_a)\alpha_\ell e^{-\alpha_\ell t_a} - \left(e^{-\alpha_\ell t_a} - e^{-\alpha_\ell t_e}\right)}{\alpha_\ell^2 \prod_{\substack{f=h\\f\neq\ell}}(\lambda_f - \lambda_\ell)}\right]\Bigg\} \ . \tag{10.12}$$

For $\delta = 3$

$$I_{i,3}(\zeta,s) = \sum_{h=1}^{i} \left\{ k(0) < \chi(\zeta;s,h) > V_d(s,h) \left(\prod_{\ell=h+1}^{i} \lambda_\ell \right) \right.$$

$$\sum_{\ell=h}^{i} \left[\frac{1 - e^{-\beta_\ell t_a} - \beta_\ell t_a e^{-\beta_\ell t_a}}{\beta_\ell^2 \prod_{\substack{f=h \\ f \neq \ell}}^{i} (\lambda_f - \lambda_\ell)} \right] \right\} + \sum_{h=1}^{i}$$

$$\left\{ k_f < \chi(\zeta;s,h) V_d(s,h) \left(\prod_{\ell=h+1}^{i} \lambda_h \right) \sum_{\ell=h}^{i} \right.$$

$$\left. \left[\frac{\alpha_\ell t_a e^{-\alpha_\ell t_a} - e^{-\alpha_\ell t_e} + e^{-\alpha_\ell (t_e + t_a)}}{\alpha_\ell^2 \prod_{\substack{f=h \\ f \neq \ell}} (\lambda_f - \lambda_\ell)} \right] \right\} . \tag{10.13}$$

For $\delta = 4$

$$I_{i,4}(\zeta,s) = \sum_{h=1}^{i} \left\{ k_f < \chi(\zeta;s,h) V_d(s,h) \left(\prod_{\ell=h+1}^{i} \lambda_h \right) \sum_{\ell=h}^{i} \right.$$

$$\left. \left[\frac{e^{-\alpha_\ell t_a} - e^{-\alpha_\ell (t_f - t_e)} - e^{\alpha_\ell (t_e + t_a)} + e^{-\alpha_\ell t_f}}{\alpha_\ell^2 \prod_{\substack{f=h \\ f \neq \ell}}^{i} (\lambda_f - \lambda_\ell)} \right] \right\} . \tag{10.14}$$

10.2 ENVIRONMENTAL DOSE COMMITMENT FROM INHALATION OF RADON DAUGHTERS

For $k = 2$,

$$D_{TB,Rn,2}^{e} = t_e \sum_{\zeta} P(\zeta,t=0)G\left(\frac{t_e}{2}\right)\hat{D}_{TB,Rn}<\chi(\zeta;Rn)> \ . \tag{10.15}$$

10.3 ENVIRONMENTAL DOSE COMMITMENT FROM EXTERNAL EXPOSURES

For $k = 3$ for external exposures from radioactive materials in air:

$$D_{\Psi,i,3}^{e} = D_{\Psi,i,3}^{e}\Big|_{p} + D_{\Psi,i,3}^{e}\Big|_{Rn} \ , \tag{10.16}$$

where

$$D_{\Psi,i,3}^{e}\Big|_{p} = \sum_{\zeta} P(\zeta,t=0)\left[\sum_{\delta=1}^{4} G(\bar{t}_\delta)\hat{D}_{\Psi,i,3} \sum_{s} I_{i,\delta}(\zeta,s)\right] \ . \tag{10.17}$$

For radon and short-lived daughters in air:

$$D_{\Psi,i,3}^{e}\Big|_{Rn} = t_e \sum_{\zeta} P(\zeta,t=0)G\left(\frac{t_e}{2}\right)\hat{D}_{\Psi,i,3}<\chi(\zeta;i)> \ . \tag{10.18}$$

Similarly the environmental dose commitment from ground deposited activity ($k = 4$):

$$D_{\Psi,i,4}^{e} = \sum_{\zeta} P(\zeta,t=0) \sum_{\delta=1}^{2} G(\bar{t}_\delta)\hat{D}_{\Psi,i,4}I_{i,\delta}(\zeta,s) \ , \tag{10.19}$$

where

$$I_{i,1}(\zeta) = \sum_{h=\ell}^{i} \left\{\left[\sum_{s} <\chi(\zeta;s,h)>V_d(s,h)\right]\left(\prod_{\ell=h+1}^{i} \lambda_\ell\right)\sum_{\ell=h}^{i}\right.$$

$$\left.\left[\frac{t_e\alpha_\ell - \left(1 - e^{-\alpha_\ell t_e}\right)}{\alpha_\ell^2 \prod_{\substack{f=\ell \\ f\neq h}}^{i} (\lambda_f - \lambda_h)}\right]\right\} \ , \tag{10.20}$$

and

$$I_{i,2}(\zeta) = \sum_{h=1}^{i} \left\{ \left[\sum_{s} <\chi(\zeta;s,h)> V_d(s,h) \right] \left(\prod_{\ell=h+1}^{i} \lambda_\ell \right) \sum_{\ell=h}^{i} \right.$$

$$\left. \left[\frac{1 - e^{\alpha_\ell(t_f - t_e)} - e^{-\alpha_\ell t_e} e^{-\alpha_\ell t_f}}{\alpha_\ell^2 \prod_{\substack{f=\ell \\ f \neq h}}^{i} (\lambda_f - \lambda_h)} \right] \right\} . \qquad (10.21)$$

10.4 ENVIRONMENTAL DOSE COMMITMENT FROM INGESTION (k = 5)

The environmental dose commitment from ingestion of contaminated foods is obtained from integration of the Eq. 9.3:

$$D_{\Psi,5}^e = \int D^P(t, \Psi) \, dt . \qquad (10.22)$$

The integration results in:

$$D_{\Psi,5}^e = P(t=0) \left[\sum_{\delta=1} G(\bar{t}_\delta) \sum_{\beta} \sum_{i} \hat{D}_{\Psi,i,5} I_\beta <C_{i\beta}(\bar{t}_\delta)> \right] \qquad (10.23)$$

where $\quad <C_{i\beta}(\bar{t}_\delta)> = \sum_{\zeta} U_{\zeta\beta} \int_{t_\delta}^{t_{\delta+1}} C_{i\beta}(t;\zeta) \, dt .$ $\qquad (10.24)$

11. UDAD COMPUTATIONAL SYSTEM

*Of the two major programs in UDAD, the first--MASTER--
computes the atmospheric concentration, ground deposition, dose
commitment, dose rate, and time-integrated dose from the data
input. From the intake rates obtained, the second program--
INTERNAL--computes the dose conversion factors for each tissue
of interest.*

The theoretical basis and default values for UDAD have been described in
the previous sections. The UDAD computer program is written in Fortran IV.
Appendix A provides a listing of this code. The execution "deck" for a sample
problem is listed in Appendix B and selected portions of the computer output
are presented in Appendix C. The sample problem utilizes a cataloged proce-
dure (collection of job control statements) which is listed in Appendix D.
This catalogued procedure is only suitable in Argonne's computer environment,
but it can serve as a guideline for other IBM installations. The UDAD code
has been organized to utilize the overlay feature of the linkage editor. It
is not necessary to run the program in this manner; but if it is desired to do
so, the required linkage editor input deck (EDT.SYSIN dataset) is listed in
Appendix E.

UDAD is divided computationally into two major programs--MASTER and IN-
TERNAL. Figure 11.1 depicts the substructure of the MASTER program, which
reads in the input data and computes the atmospheric concentration, ground
deposition, dose commitment, dose rate, and time-integrated dose. The calcu-
lations are printed as a series of tables, and selected values are stored in
disk files for subsequent use by the independent plotting programs CONCPLOT
and CONTOUR. The function of each subroutine in MASTER is described in
Table 11.1.

Table 11.1. Functions of MASTER Subprograms

Subprogram	Function
ACT	Performs multiplication of a matrix and a vector.
ACTDR1	Computes 222Rn decay and daughter products ingrowth.
ACTDR2	Computes factors in a matrix form for radioactive decay ingrowth and physical removal.
AFUNC	Computes standard deviation of plume concentration distribution in vertical direction.
ANC4	A utility numerical integration subroutine.
BLOCK DATA	Initializes program variables and arrays.
CONC	Computes average air and ground concentrations for a specific time interval.
DDEP	Computes source depletion factor.
DFUNC	Double precision version of AFUNC.
DOCOMT	Computes dose commitment values.
DOSAGE	Computes time-integrated dose and dose rate.
DOSPOP	Computes population dose commitment.
EVPDOS	Computes environmental dose commitment.
FERR	Evaluates function #1 for source depletion integration.
FERR1	Evaluates function #2 for source depletion integration.
FODOSE	Computes ingestion dose commitments, time-integrated dose, and dose rate.
FOOD	Computes radionuclide concentrations in foodstuff.
GROUND	Computes time dependent and time-integrated ground contamination values.
HEADER	Generates page headers.
HT	Function to compute effective stack height.
INTEG	Performs numerical integration for source depletion.
KSZFC	Determines if non-zero particle size activity fraction has been assigned for a given particle size index.
MAIN (UDAD)	Main driver of program. Initializes program variables, reads input, prints output, writes disk files.
NSNE	Function that selects proper series of dose conversion factors to be used for a given radionuclide.
PART1	Secondary driver for first part of UDAD: prints all input parameters, executes dispersion calculations.
POLUT	Computes ground-level atmospheric concentration from dispersion of source.
TAILPS	Computes suspension rate of wind blown particulates from an area source.
TAIRR	Computes time dependent and time-integrated air concentration.
VEGFOD	Computes radionuclide concentrations in vegetation.

The INTERNAL program computes the conversion factors for dose commitment, dose rate, and time-integrated dose from the inhalation and ingestion of radioactive materials. Radioactive intake rates are obtained from MASTER, and INTERNAL computes the dose factors for each tissue of interest. The substructure of the INTERNAL code is depicted in Figure 11.2, and the function of each subroutine is described in Table 11.2.

11.1 DESCRIPTION OF INPUT DATA

Input data for the UDAD code can be classified in five groups: source data, receptor data, meteorological data, pollutant data, and population data.

Source Data

Both area and point sources may be specified. For a large-area source it is recommended that one use a series of smaller area sources. This can be done automatically via the IDSQ parameter, which will break up a selected source into a specified number of equal squares. For each source the location, area, effective release height, average annual emission velocity, and the pollutant characteristics must be input. A maximum of 80 sources may be specified.

Receptor Data

The normal UDAD default is 240 receptor locations corresponding to the intersections in a grid pattern of 16 wind sectors and 15 radial distances. Any set of 0-15 radial distances in the range 0.1 to 99.9 km may be selected. A default series of 0.1 to 80 km is built into the program. In addition to the regular receptors, 0-60 selected extra receptor locations may be input by the user. For each selected extra receptor only one food item for ingestion dose estimate is allowed.

Meteorological Data

The stability wind-rose data, which describes the relative frequency of occurrence for each wind direction, wind speed class, and stability category
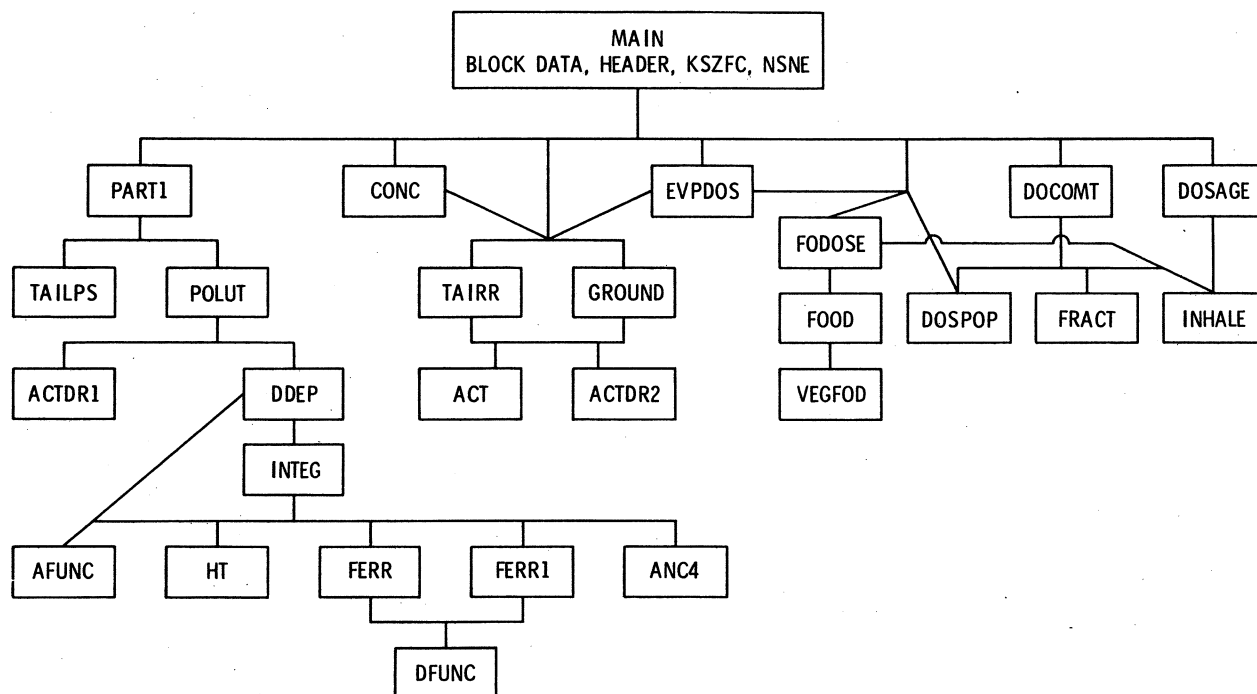
Fig. 11.1. Structure of MASTER.
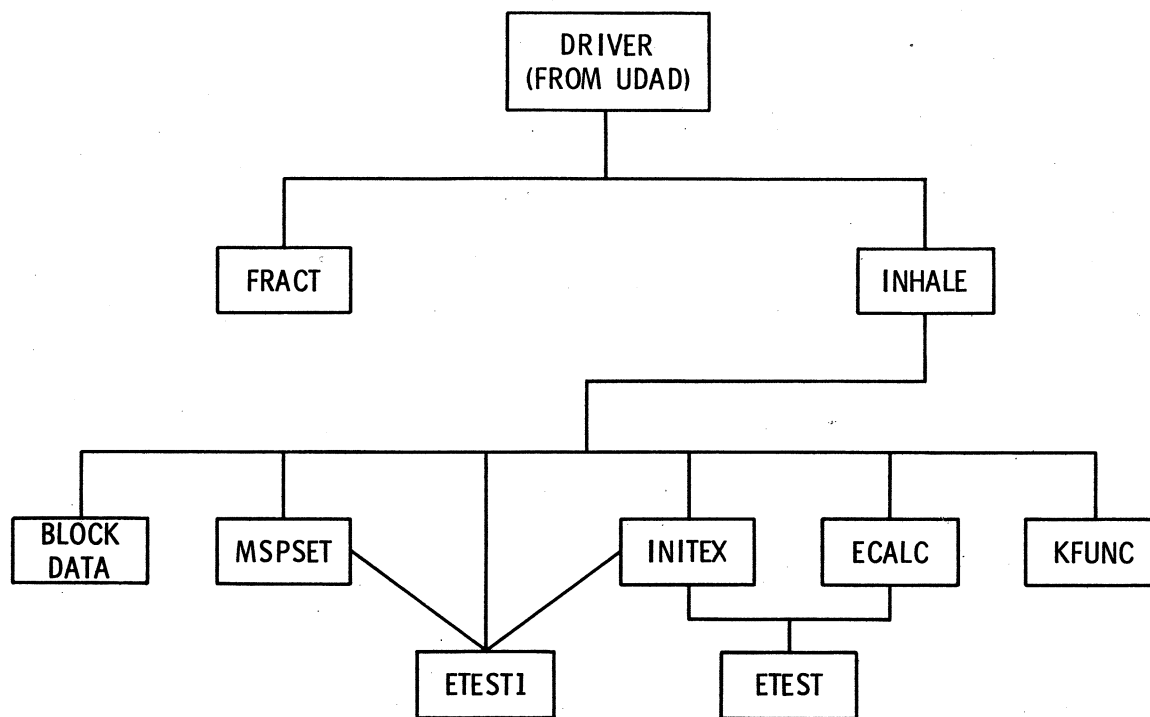
Fig. 11.2. Structure of INTERNAL.

Table 11.2. Functions of INTERNAL Subroutines

Subprogram	Function
BLOCK DATA	Initializes program variables and arrays.
ECALC	Evaluates and saves exponentials used by INHALE.
ETEST	Function to test for exponential overflow.
ETEST1	Function to evaluate expression: $[1 - \exp(-\lambda T)]/\lambda$
INITEX	Converts input half-life values to decay constants, calculates effective decay constants.
INHALE	Main driver of program; computes internal dose commitment factors, time-integrated dose, and dose rate.
KFUNC	Function to control respiratory tract flow.
FRACT	Computes deposited fraction in the lung subcompartments as a function of particle size.
MSPSET	Evaluates quantities needed for multiple subpath calculations.

combination as observed for the region, must be specified. The complete set of stability wind-rose data consists of 576 frequency values: a combination of 6 stability categories, 16 wind directions, and 6 wind speed classes.

Pollutant Data

For particulate pollutants the particle-size distribution, density, and deposition velocity must be specified. Up to five particle sizes and five size distributions may be input by the user.

Population Data

Population data for the 240 sector-segments corresponding to the 16 wind sectors and 15 radial distances may be specified. They are used for population-dose calculations.

11.2   INPUT DATA INSTRUCTIONS

This section describes the problem input data for the UDAD code.   The first card always contains a single parameter, ISTEP, in column 1.   ISTEP allows the calculations to be broken into multiple independent jobs.   This is useful for cases involving many sources where computer time requirements could become excessive.   In addition, it is possible to run several types of dosimetry calculations without rerunning the expensive dispersion computations. The allowed ISTEP values are:

0, do complete UDAD as one job.

1, stop at end of dispersion calculations; save all data.

2, resume UDAD where ISTEP=1 left off.

3, same as ISTEP=2 plus read in new dosage parameter values.

4, same as ISTEP=0 plus save all data as in ISTEP=1.

All other UDAD data is input via the unformatted NAMELIST READ statement.   The following is a direct quote from the IBM Fortran IV Language manual:

Input data must be in a special form in order to be read using a NAMELIST list.   The first character in each record to be read must be blank.   The second character in the first record of a group of data records must be an &, immediately followed by the NAMELIST name.   The NAMELIST name must be followed by a blank and must not contain any embedded blanks.   This name is followed by data items separated by commas.   (A comma after the last item is optional.)   The end of a data group is signaled by &END.

The form of the data items in an input record is:

symbolic name = constant

The symbolic name may be an array element name or a variable name.   Subscripts must be integer constants.   The constant may be integer, real, literal, complex, or logical.   (If the constants are logical, they may be the form of T or .TRUE.   and F or .FALSE)

array name = set of constants (separated by commas)

The set of constants consists of constants of the type integer, real, literal, complex, or logical. The number of constants must be less than or equal to the number of elements in the array. Successive occurrences of the same constant can be represented in the form k*constant, where k is a nonzero integer constant specifying the number of times the constant is to occur.

The variable names and array names specified in the input data set must appear in the NAMELIST list, but the order is not significant. A name that has been made equivalent to a name in the input data cannot be substituted for that name in the NAMELIST list. The list can contain names of items in COMMON but must not contain dummy argument names.

Each data record must begin with a blank followed by a complete variable or array name or constant. Embedded blanks are not permitted in names or constants. Trailing blanks after integers and exponents are treated as zeros.

A list and description of all NAMELIST input variables is presented in Table 11.3. There are two such sets: INDATA and NEWSET. NEWSET is used only in conjunction with ISTEP = 3 to input new parameter values. All NEWSET members are a subset of the INDATA list and are marked by an asterisk preceding the symbolic name. Array variables are indicated by a Fortran dimension in parentheses following the symbolic name. Variable types follow default Fortran first letter conventions except as indicated immediately below the symbolic name. UDAD default values will be used for any variable not included in the NAMELIST input.

11.3   OUTPUT DATASETS

UDAD uses three output data sets: Fortran reference numbers 8, 9, 10. This is in addition to the regular Fortran print file, reference number 6. The output datasets are used as follows:

FT08F001 Binary data used to construct concentration and working level

Table 11.3. NAMELIST Variables

Symbolic Name	Description
&INDATA	This is the 2nd data deck card if ISTEP=0, 1, or 4.
&NEWSET	This is the 2nd data deck card if ISTEP=3
*BSV (6) (i)	Concentration factor for plant uptake of nuclide i from soil, pCi/kg (plant)/pCi/kg (soil). Default values: i=1 U238 2.5E-3, i=2 U234 2.5E-3, i=3 Th230 4.2E-3 i=4 Ra226 3.1E-4, i=5 Pb210 6.8E-2, i=6 Po210 1.5E-1
*DFACT	Decontamination factor for human consumed vegetation. Default value = 0.5.
DM	Annual average mixing depth, m. Default = 850.
*DV (2) (i)	Pastures and vegetation yields, kg/m2. Defaults: i=1 pastures 0.75, i=2 vegetation 2.0.
*E(10,12) (i,j)	Effective energy absorbed per disintegration (MEV*REM/DIS*RAD), where i and j denote the radionuclide and organ, respectively. Default values are based on ICRP reports.

j	Organ or body part
1	Nasopharyngeal
2	Tracheobronchial
3	Pulmonary
4	Whole body
5	Bone
6	Kidney
7	Liver
8	Stomach
9	Small intestine
10	Upper large intestine
11	Lower Large intestine
12	Lymph nodes

Default values:

j\i	U238	U234	Th230	Ra226	Pb210	Po210
1	4.3E+1	4.9E+1	4.8E+1	1.1E+2	6.1E-1	5.5E+1
2	4.3E+1	4.9E+1	4.8E+1	1.1E+2	4.8E-1	5.5E+1
3	4.3E+1	4.9E+1	4.8E+1	1.1E+2	8.3E+0	5.5E+1
4	4.3E+1	4.9E+1	4.8E+1	1.1E+2	5.2E+0	5.5E+1
5	2.2E+2	2.4E+2	2.4E+2	1.1E+2	2.9E+1	2.8E+2
6	4.3E+1	4.9E+1	4.8E+1	1.1E+2	1.0E+1	5.5E+1
7	4.3E+1	4.9E+1	4.8E+1	1.1E+2	1.0E+1	5.5E+1
8	4.3E-1	4.8E-1	4.7E-1	4.8E-1	2.7E-2	5.3E-1
9	4.3E-1	4.9E-1	4.7E-1	4.8E-1	4.5E-2	5.3E-1
10	4.3E-1	4.8E-1	4.7E-1	4.8E-1	1.9E-2	5.3E-1
11	4.3E-1	4.8E-1	4.7E-1	4.8E-1	1.9E-2	5.3E-1
12	4.3E+1	4.9E+1	4.8E+1	1.1E+2	2.5E+1	5.5E+1

*FCON (6,5) (i,j)

Stable element transfer data, day/kg, where i and j denote the radionuclide and the food item respectively. j values: 1=beef, 2=milk, 3=poultry, 4=eggs, 5=vegetation

Default values:

j\i	U238	U234	Th230	Ra226	Pb210	Po210
1	3.4E-4	3.4E-4	2.0E-4	4.0E-3	2.9E-4	1.2E-2
2	6.1E-4	6.1E-4	5.0E-6	4.5E-4	2.6E-4	1.4E-4
3	4.0E-3	4.0E-3	4.0E-3	5.0E-4	2.0E-3	4.0E-3
4	2.0E-3	2.0E-3	2.0E-3	2.0E-5	2.0E-3	1.8E-2
5	2.0E+0	2.0E+0	3.0E+1	5.0E+1	1.0E+2	5.0E+2

Table 11.3. Continued

Symbolic Name	Description

*F1 (10)
(i)

Fraction of radionuclide i passing from GI tract to the blood. Default values are based on ICRP2. Defaults:
i=1 U238 1.0E-2, i=2 U234 1.0E-2, i=3 Th230 1.0E-4,
i=4 Ra226 3.0E-1, i=5 Pb210 8.0E-2, i=6 Po210 6.0E-2

*F2P (10,4)
(i,j)

Fraction of radionuclide i passing from blood to body organ j. j values: 1=whole body, 2=bone, 3=kidney, 4=liver. Defaults:

j\i	U238	U234	Th230	Ra226	Pb210	Po210
1	1.0E+0	1.0E+0	1.0E+0	5.4E-1	1.0E+0	1.0E+0
2	1.1E-1	1.1E-1	7.0E-1	5.4E-1	2.8E-1	1.0E-1
3	1.1E-1	1.1E-1	5.0E-2	2.0E-3	1.4E-1	7.0E-2
4	0.0	0.0	5.0E-2	4.0E-4	8.0E-2	1.7E-1

*F2PM (16)

Multiple subpath values of F2P, see MSPTAB. Defaults:

2.9E-1	1.1E-1	4.0E-2	2.0E-2
2.9E-1	1.1E-1	4.0E-2	2.0E-2
0.0	0.0	0.0	0.0
0.0	0.0	0.0	0.0

*FG

Grazing factor, default=0.5.

*FOODIN (2,3)
(i,j)

Animal food ingestion rate, kg/day, where i and j denote the food category and animal type respectively. Defaults:

i\j	beef cattle	milk cows	poultry
water	50	60	0.3
pasture	50	50	0.12

FREQ (16,6,6)
(i,j,k)

Annual relative frequency of occurence for wind direction i, wind speed class j, and stablity class k. For each stability class and wind speed the frequencies are entered in a clockwise direction beginning with the north sector. No defaults; values must be input.

*FV (2)
(i)

Fraction of deposition retained on plants. Default values: i=1 pasture 0.2, i=2 vegetation 0.2.

GROUPN(5,9)
(i,j)

Any desired combination of 20 letters and numbers which will serve as an identifier on the printed output for the jth source type, i.e., mine, dryer, etc. (Card entry consists of groups of 4 characters, each enclosed in single quotation marks followed by a comma.)

IADD

Number of extra receptors, allowable range 0-60, default=0.

IDSQ (3,6)
(i,j)

Identifies area sources to be broken up into equal size squares: i=1, SOURCE(10,k) or four digit identifier for kth source; i=2, number of squares in EW direction, i=3, number of squares in NS direction; all for jth source selected to be broken up. No defaults.

IDTAIL (5)
(i)

Identification of up to 5 types of area source where the UDAD wind errosion equation will be used for particulate source estimation. Each ith value must be identical to the source type index of SORCE, i.e., the 2nd integer of SORCE(10,j) for the jth source. Area sources so selected may specify zero emission rate for all pollutants except Rn222. No defaults.

Table 11.3. Continued

Symbolic Name	Description

*IFODOS (60)
(i)

Food pathway index for the ith extra receptor. 0=none, 1=meat, 2=milk, 3=poultry & eggs, 5=vegetation. Default=0.

IPOP (15,16)
(i,j)

Population of sector-segment centered at ith radial distance and jth direction.

*IPSOL (10)
(i)

Solubility class (1=Y, 2=W, 3=D) for ith radionuclide.
Defaults: i=1 U238 1, i=2 U234 1, i=3 Th230 1,
          i=4 Ra226 2, i=4 Pb210 2, i=6 Po210 2.

*IRHO (6)

Specifies the six XRHO indices to be used for dosimetry tables. Default: 1, 3, 7, 8, 12, 15 corresponding to 0.1, 1, 5, 10, 50, 80 km.

*IYR (10)

Selects end year for intervals in time-integrated dose and dose rate calculations. Default: 1, 3, 5, 7, 10, 15, 20, 30, 50, 70 years.

*JC (9)
(i)

Program control flags: 0 turns action off, 1 turns it on.
Defaults = 0.
i=1, writes disk file for concentration plots.
i=2, writes disk file for isopleth plots.
i=3, prints EFFECTIVE DISPERSION FACTOR tables.
i=4, prints CONCENTRATION/MPC tables.
i=5, prints dose commitment tables.
i=6, prints time-integrated dose & dose rate tables.
i=7, currently not in use.
i=8, prints INDIVIDUAL SOURCE CONCENTRATION tables.
i=9, currently not in use.

KRHO

Specifies number of radial distances to be used for regular receptor grid. Range 0-15, default = 15.
If set to zero, only extra receptors will be used, which is frequently a convenient option.

*LON (10,4)
REAL (i,j)

Effective half-life in days for radionuclide i and organ j. j values: 1=whole body, 2= bone, 3=kidney, 4=liver. Default values based IRCP reports. Defaults:

j\i	U238	U234	Th230	Ra226	Pb210	Po210
1	1.0E+2	1.0E+2	5.7E+4	4.0E-1	1.2E+3	2.5E+1
2	3.0E+2	3.0E+2	7.3E+4	4.0E-1	2.4E+3	2.0E+1
3	1.5E+1	1.5E+1	2.2E+4	1.0E+1	4.9E+2	4.6E+1
4	0.0	0.0	5.7E+4	1.0E+1	1.5E+3	3.2E+1

*LONM (16)
Real

Multiple subpath values of LON, see MSPTAB. Defaults:
4.95E+0 5.78E+1 6.93E+2 5.33E+3
4.95E+0 5.78E+1 6.93E+2 5.33E+3
0.0   0.0   0.0   0.0
0.0   0.0   0.0   0.0

*LR (10)
Real (i)

Radiological half-lifes in days for radionuclides of interest. Defaults:
i=1 U238 1.6E12, i=2 U234 9.1E7, i=3 Th230 2.9E7
i=4 Ra226 5.9E5, i=5 Pb210 7.1E3, i=6 Po210 1.4E2

METSET (4)
Real*8

Any desired combination of 32 letters and numbers which will serve as an identifier on the printed output for the source of the meteorological data set. (Card entry starts with a single quotation mark and ends with a single quotation mark followed by a comma.)

Table 11.3. Continued

Symbolic Name	Description
*MPC (7,5) Real(i,j)	Maximum permissible concentration (or any desired limit) for normalization on the isopleth concentraion map, pCi/m3, for radionuclide i and organ j. Default values based on ICRP2 values. j values: 1=whole body, 2=bone, 3=lung, 4=kidney, 5=liver. Defaults:

i\j	1	2	3	4	5
U238	6.0E+2	2.0E+2	5.0E+1	3.0E+1	0.0
U234	6.0E+2	2.0E+2	4.0E+1	4.0E+2	0.0
Th230	5.0E+0	8.0E-1	3.0E+0	2.0E+0	7.0E+0
Ra226	2.0E+1	1.0E-1	0.0	0.0	0.0
Pb210	4.0E+2	7.0E+1	8.0E+1	4.0E+1	1.0E+2
Po210	2.0E+3	2.0E+3	7.0E+1	2.0E+2	6.0E+2
Rn222	0.0	0.0	3.0E+3	0.0	0.0

Symbolic Name	Description
*MSPTAB (10,4) (i,j)	Multiple subpath table for radionuclides i and organs j where multiple sets of F2P and LON values are required. A zero value indicates no subpath, units value (1-9) gives number of additional subpaths, and value/10 is entry index in F2P and LON arrays. j values: 1=whole body, 2=bone, 3=kidney, 4=liver. Defaults:

j\i	U238	U234	Th230	Ra226	Pb210	Po210
1	0	0	0	14	0	0
2	0	0	0	54	0	0
3	0	0	0	0	0	0
4	0	0	0	0	0	0

Symbolic Name	Description
*NNUC	Total number of radionuclides of interest. UDAD allowable range is 1-6, default is 6.
NSORCE	Total number of sources. Input value must be actual number described via SORCE parameter. If IDSQ feature is used, UDAD will adjust to a corrected NSORCE. The maximum number of sources, including IDSQ components, is 80.
OPTIME	Plant operation lifetime, years. Default=15.
PACT (4,5) (i,j)	Activity in pCi/g of radionuclide i of particle size<20 um diameter of area source j. The j index corresponds to IDTAIL(j). i values: 1=U238, 2=Th230, 3=Ra226, 4=Pb210.
PDEN (5)	Densities of five specified particle source indices, g/cm3. Defaults: 8.9, 2.4, 2.4, 2.4, 2.4.
*PFIN (8) (i)	Fraction of ith food produced within the region of interest that is consumed by the local population in the region. i values: 1=meat, 2=milk, 3=poultry, 4=eggs, 5=vegetation, 6-8 not assigned. Defaults: all=1.0.
*PGTH (4) (i)	Population growth rate = population at year Y(i)/population at the reference year Yo when sources start to release. i=1, Y(i) = Yo + 1 i=2, Y(i) = Yo + (OPTIME + 1)/2 i=3, Y(i) = Yo + OPTIME + 1 i=4, Y(i) = Yo + OPTIME + YEVD/2 + 1 Defaults: all=1.0.
PHALF	Radionuclide removal half life from soil in years. Default=50.

Table 11.3. Continued

Symbolic Name	Description
PTAIL (7,5) (i,j)	Propterty of soil or tailings for the jth type of area source where j index corresponds to IDTAIL(j). i values: i=1, density of suspended particulates, gm/cm3. i=2, median diameter of the grain, cm. i=3, a dimensionless coefficient for grains with median diameter above 100 um, A=0.1. i=4, height above surface where wind speed measured, cm. i=5, surface roughness height, or height above surface where wind speed is zero, cm. i=6, particle mass percentage of soil < 20 um in diameter. i=7, water content in percent by weight. Defaults:

j\i	1	2	3	4	5	6	7
1	2.4	0.03	0.1	100.0	1.0	3.0	0.1
2	0	0	0	0	0	0	0
3	0	0	0	0	0	0	0
4	0	0	0	0	0	0	0
5	0	0	0	0	0	0	0

Symbolic Name	Description
PTSZ (5)	Activity particle sizes, diameter in microns. Defaults=0.
PTSZFC (5,5) (i,j)	Particle size activity fraction for ith size and jth source. The i and j indices correspond to PTSZ(i) and PDEN(j) respectively. Defaults=0.
PTSZ2Ø (5) (i)	Activity fraction of suspended particulates with particle size < 20 um for ith area source. The i index corresponds to IDTAIL(i). Defaults: all=0.4.
*PWFOD (60) (i)	Amount of kth food item produced at added receptor i/ total kth food item produced within the region of interest. Defaults: all=1.0.
REGION (6)	Any desired combination of 24 letters and numbers which will serve as in identifier of the overall problem on the printed output. (Card input format is the same as for METSET.)
RFI	Average occupancy factor for the population inside a structure for inhalation of Rn222 daughters. Default=1.0.
*RFIE	Average occupancy factor inside a structure for protection against external radiation. Default=0.583.
*RHO (2) (i)	Effective surface density of soil for growing pastures and and vegetation, kg/m2. Defaults: i=1 pastures 2.4E2, i=2 vegetation 2.4E2.
*RSALF	Resuspension factor decay half life in years, default=0.137.
*RSLIM	Deposition velocity corresponding to the input resuspension factors SUFI and SUFF. Default=0.01 m/sec.
*SHIED	External radiation shielding factor for inside of a structure. Default=0.5.
SLIM	Minimum settling velocity to account for plume tilting, m/sec. Default = 0.01.
SLIP (5) (i)	Slip correction factor, for ith particle size, defaults = 1.0.

Table 11.3. Continued

Symbolic Name	Description
SOURCE (12,80) (i,j)	Specification parameters for the jth source. i values: i=1, horizontal (EW) coordinate of source, km. i=2, vertical (NS) coordinate of source, km. i=3, effective release height of source, m. i=4, release area of source, km2 (zero for a point source). i=5, annual average U238 emission rate, Ci/year. i=6, annual average Th230 emission rate, Ci/year. i=7, annual average Ra226 emission rate, Ci/year. i=8, annual average Pb210 emission rate, Ci/year. i=9, annual average Rn222 emission rate, Ci/year. i=10, four digit integer for source j identification where the 1st integer is the source group index, the 2nd integer is the source type index, the 3rd & 4th integers represent the nth number of source falling into this source category. i=11, particle density index, corresponds to PDEN(k). i=12, exit velocity of source, m/sec.
SORCID (5,9) (i,j)	Any desired combination of 20 letters or numbers which will serve as an identifer on the printed output for the jth source group where j equals the 1st digit of SORCE(10,k) for the kth source. (Card entry is the same format as for GROUPN.)
*SUFF	Final resuspension factor. Default=1.0E-9/m.
*SUFI	Initial resuspension factor. Default=1.0E-5/m.
*TC (2) (i)	Plant exposure time, days. Defaults: i=1 pastures 30, i=2 vegetation 60.
*TW (2) (i)	Weathering removal half life, days. Defaults: i=1 pastures 14, i=2 vegetation 14.
VDEP (5) (i)	Deposition velocity, m/sec, for particle size PTSZ(i). Defaults: all=0.01.
*XIN (7) (i)	Maximum individual food consumption rate, kg/day. See XING for defaults.
*XING (7) (i)	Average individual food consumption rate, kg/day. Defaults:

	XIN	XING
i=1, meat	0.3	0.26
i=2, milk	0.85	0.33
i=3, poultry	0.2	0.1
i=4, eggs	0.08	0.08
i=5, vegetation	0.77	0.28

Symbolic Name	Description
XNAME (4,60) REAL*8 (i,j)	Any desired combination of 32 letters and numbers which which will serve as an identifer on the printed output for extra receptor j. (Card input format is the same as for GROUPN except use 8 character groups).
XRECEP (3,60) (i,j)	Coordinates and height of jth extra receptor. i=1, horizontal (EW) coordinate, km. i=2, vertical (NS) coordinate, km. i=3, height in m.
XRHO (15)	Fifteen radial distances to be used for regular receptor grid. Defaults: 0.1, 0.5, 1, 2, 3, 4, 5, 10, 20, 30, 40, 50, 60, 70, 80 km. (Note that actual numer of XRHO values used is set by KRHO).
*YDOC	Number of years to be used for internal dose commitment conversion factors. Default=50.
*YEVD	Number of years to be used for environmental dose commitment calculations. Default=100.

plots vs. distance. In the case of a multiple step UDAD job
(ISTEP>0), this dataset also contains a dump of all data needed
to restart the program.

FT09F001   EBCDIC file of log (concentration/MPC) and point coordinates
used to construct isopleth plots. All records are 80 bytes.

FT10F001   Special print file, used to produce effective dispersion factor
tables, 133 byte records.

11.4   PLOTTING PROGRAMS

CONCPLOT Program

CONCPLOT is a Fortran IV main program that uses the proprietary software
package DISSPLA. The only input required is the FT08F001 disk file generated
by UDAD. Log-log plots of distance vs. concentration in air and on the ground
are produced for ^{238}U, ^{226}Ra, ^{210}Pb, and ^{222}Rn. A working-level plot is also
prepared. Five curves are generated on each plot for directions theta,
north, east, south and west, where theta is the direction of maximum dispersion.

CONTOUR Program

CONTOUR is a PL/1 program that serves as a data selector and generator
for CONTOUR.BLACKBOX, an Argonne version of a proprietary contour mapping
program. Input data are the FT09F001 disk file generated by UDAD and a 2- to
6-card user-supplied deck (ISO.SYSIN dataset of cataloged procedure). The
output is one or two isopleth plots of log of concentration divided by MPC for
selected tissues and radionuclides.

Input Data Instructions for CONTOUR

The first card indicates grid spacing and contour interval for the one or
two isopleth plots produced for each selected organ and nuclide. Leave grid
field blank to obtain default values; set grid field negative to omit plot
type. First card also includes seldom-used options for including the extra

receptors for contour generation and for linear instead of quadratic fit in interpolations.

```
1st card, PL/1 Format (4 F(5,2), 2 (X(4), F(1))):
   Col   1- 5   Grid #1, default = 2 km squares.
         6-10   Contour interval #1, default = 0.25 log units.
        11-15   Grid #2, default = 20 km squares.
        16-20   Contour interval #2, default = 0.50 log units.
           25   Include additional receptors if = 1, default = 0.
           30   Linear interpolation if = 1, quadratic default if = 0.


Cards 2-6, P1/1 Format (A(6), 7 (X(1), A(5))):
   Col   1-6    'BODY', 'BONE', 'LUNG', 'KIDNEY', OR 'LIVER'.
         8-48   1 TO 7 nuclides in any order: 'U238', 'U234', 'TH230',
                'RA226', 'PB210', 'PO210', 'RN222'.
```

Example of 20 km squares only for ^{238}U and ^{230}Th on whole body, ^{226}Ra on bone, and ^{222}Rn on lung:

```
//ISO.SYSIN  DD  *
  -1.
BODY    U238  TH230
BONE    RA226
LUNG    RN222
```

12.   SAMPLE PROBLEM DESCRIPTION

A sample problem was selected for illustrating the actual application of the UDAD program. The sample problem considered is a typical uranium mill processing 1800 metric tons per day of an ore containing an average of 0.16% U_3O_8.

The procedures for calculating the source terms (annual release rates) utilized as input in UDAD are presented in the following subsections. The source terms are based on the selected mill operational parameters given in Table 12.1, and the calculated source terms are summarized in Table 12.2.

12.1   ORE PAD AND GRINDING OPERATIONS

Radon

The activity of ^{222}Rn available for release from the decay of ^{226}Ra from each gram of ore during storage on the ore pad is

$$^{222}\text{Rn activity} = EC_{Ra}\lambda T , \tag{12.1}$$

where   E is the emanating power, 0.2,

C_{Ra} is the concentration of ^{226}Ra in ore, 450 pCi/g,

λ is the decay constant for ^{222}Rn, 0.18/day, and

T is the storage time on ore pad, 10 days.

Since the ore processing rate is 1800 MT/day, the ^{222}Rn emission rate is:

$$0.2 \times 450 \times 0.181/\text{day} \times 10 \text{ days } \frac{\text{pCi}}{\text{g}} \times (1800 \times 365) \frac{\text{MT}}{\text{yr}}$$

$$\times 10^6 \frac{\text{g}}{\text{MT}} \times 10^{-12} \frac{\text{Ci}}{\text{pCi}} = 107 \text{ Ci/yr} . \tag{12.2}$$

Table 12.1. Principal Characteristic
Operational Parameters of the
"Problem Mill" Utilized for the
Calculation of Source Terms

Parameter	Value
Ore quality, U_3O_8	0.16 %
Ore activity, ^{238}U	450 pCi/g
^{230}Th	450 pCi/g
^{226}Ra	450 pCi/g
^{210}Pb	450 pCi/g
Ore process rate	1800 MT/yr
Operating days per year	365 days
Operating lifetime	15 years
Ore storage time	10 days
Dry tailing density	2.4 g/cm^3
Tailing activity, ^{238}U	45 pCi/g
^{230}Th	450 pCi/g
^{226}Ra	450 pCi/g
^{210}Pb	450 pCi/g
Tailing beach area	5×10^5 m^2
Yellowcake drying & packaging stack effluent, U_3O_8	0.7 kg/day

Table 12.2. Source Terms for the Problem Mill

| Emission Source | Emission Coordinates | | | Area m^2 | Emission Rate, Ci/yr | | | | |
	x,m	y,m	z,m		U-238	Th-230	Ra-226	Pb-210	Rn-222
Ore pad and grinding	0.0	0.1	5	0[a]	$1.36×10^{-3}$	$1.36×10^{-3}$	$1.36×10^{-3}$	$1.36×10^{-3}$	107
Product drying and packaging	0	0	15	0[a]	$7.2×10^{-2}$	$3.58×10^{-3}$	$1.43×10^{-4}$	$1.43×10^{-4}$	0.0
Tailings[b]	130	-270	0	$3.13×10^4$	$8.73×10^{-4}$	$1.18×10^{-2}$	$1.24×10^{-2}$	$1.24×10^{-2}$	$4.38×10^2$
	310	-270	0	$3.13×10^4$	$8.73×10^{-4}$	$1.18×10^{-2}$	$1.24×10^{-2}$	$1.24×10^{-2}$	$4.38×10^2$
	490	-270	0	$3.13×10^4$	$8.73×10^{-4}$	$1.18×10^{-2}$	$1.24×10^{-2}$	$1.24×10^{-2}$	$4.38×10^2$
	670	-270	0	$3.13×10^4$	$8.73×10^{-4}$	$1.18×10^{-2}$	$1.24×10^{-2}$	$1.24×10^{-2}$	$4.38×10^2$
	130	-90	0	$3.13×10^4$	$8.73×10^{-4}$	$1.18×10^{-2}$	$1.24×10^{-2}$	$1.24×10^{-2}$	$4.38×10^2$
	310	-90	0	$3.13×10^4$	$8.73×10^{-4}$	$1.18×10^{-2}$	$1.24×10^{-2}$	$1.24×10^{-2}$	$4.38×10^2$
	490	-90	0	$3.13×10^4$	$8.73×10^{-4}$	$1.18×10^{-2}$	$1.24×10^{-2}$	$1.24×10^{-2}$	$4.38×10^2$
	670	-90	0	$3.13×10^4$	$8.73×10^{-4}$	$1.18×10^{-2}$	$1.24×10^{-2}$	$1.24×10^{-2}$	$4.38×10^2$
	130	90	0	$3.13×10^4$	$8.73×10^{-4}$	$1.18×10^{-2}$	$1.24×10^{-2}$	$1.24×10^{-2}$	$4.38×10^2$
	310	90	0	$3.13×10^4$	$8.73×10^{-4}$	$1.18×10^{-2}$	$1.24×10^{-2}$	$1.24×10^{-2}$	$4.38×10^2$
	490	90	0	$3.13×10^4$	$8.73×10^{-4}$	$1.18×10^{-2}$	$1.24×10^{-2}$	$1.24×10^{-2}$	$4.38×10^2$
	670	90	0	$3.13×10^4$	$8.73×10^{-4}$	$1.18×10^{-2}$	$1.24×10^{-2}$	$1.24×10^{-2}$	$4.38×10^2$
	130	270	0	$3.13×10^4$	$8.73×10^{-4}$	$1.18×10^{-2}$	$1.24×10^{-2}$	$1.24×10^{-2}$	$4.38×10^2$
	310	270	0	$3.13×10^4$	$8.73×10^{-4}$	$1.18×10^{-2}$	$1.24×10^{-2}$	$1.24×10^{-2}$	$4.38×10^2$
	490	270	0	$3.13×10^4$	$8.73×10^{-4}$	$1.18×10^{-2}$	$1.24×10^{-2}$	$1.24×10^{-2}$	$4.38×10^2$
	670	270	0	$3.13×10^4$	$8.73×10^{-4}$	$1.18×10^{-2}$	$1.24×10^{-2}$	$1.24×10^{-2}$	$4.38×10^2$

[a] Point source is assumed.

[b] 70% of particulates emitted with median size of 35 μ (10 - 80 μ). 30% of particulates emitted with median size of 5 μ (0 - 10 μ).

Particulates

The amount of particulates **released** from ore pad storage, crushing, and grinding is based on the following assumptions:

From the ore pad,	1 MT/year
From the crushing operation,	0.25 g/MT of ore
From the grinding operation,	0.15 g/MT of ore

The total annual release is:

$$1 \text{ MT/year} + (0.25 + 0.15) \text{ g/MT} \times 1800 \text{ MT/day} \times 365 \text{ days/year}$$

$$\times 10^{-6} \text{ MT/g} = 1.26 \text{ MT/year} . \qquad (12.3)$$

The activity released annually is:

$$1.26 \text{ MT/year} \times 10^6 \text{ g/MT} \times 450 \text{ pCi/g} \times 10^{-12} \text{ Ci/pCi}$$

$$\times 2.4 \left(\frac{\text{specific activity of released fraction}}{\text{average specific activity of ore}} \right)$$

$$= 1.36 \times 10^{-3} \text{ Ci/year} . \qquad (12.4)$$

This is the activity of each of the radionuclides ^{238}U, ^{234}U, ^{230}Th, ^{226}Ra, ^{210}Pb, and ^{210}Po. It is assumed to be in the form of particulates having an activity median diameter of 1.0 μm.

12.2 YELLOWCAKE DRYING AND PACKAGING

Radon

The radon release from the drying and packaging processes is negligible.

Particulates

Yellowcake is assumed to contain ^{238}U, ^{230}Th, ^{226}Ra, ^{210}Pb, and ^{210}Po in the following ratio: 1:0.05:0.002:0.002:0.002.

Dust emission during product drying and packaging is controlled by passing the off-gas from the drying and packaging areas through a dust separation system before the gas is discharged through a roof stack.

Dust emission is assumed to be 0.7 kg U_3O_8 per day having an activity median diameter of 1.0 μm.

The ^{238}U emission rate is:

$$700 \frac{g}{day} \times 365 \frac{day}{yr} \times \frac{0.85 \text{ g U}}{\text{g } U_3O_8} \times 3.33 \times 10^{-7} \frac{Ci}{g} = 7.2 \times 10^{-2} \frac{Ci}{yr} . \quad (12.5)$$

The ^{230}Th emission rate is:

$$7.2 \times 10^{-2} \frac{Ci}{yr} \times 0.05 = 3.6 \times 10^{-3} \frac{Ci}{yr} . \quad (12.6)$$

The ^{226}Ra, ^{210}Pb, and ^{210}Po activity is:

$$7.2 \times 10^{-2} \frac{Ci}{yr} \times 0.002 = 1.4 \times 10^{-4} \frac{Ci}{yr} . \quad (12.7)$$

12.3 TAILINGS

Radon

The radon flux from beach area (i.e., area not covered by solution) is assumed on the average to be 1.0 pCi ^{222}Rn/m^2-sec per pCi ^{226}Ra/g of tailings. With a ^{226}Ra concentration of about 450 pCi/g in the tailings the annual rate of radon release is:

$$450 \frac{\text{pCi } ^{226}\text{Ra}}{\text{g tailing}} \times 1.0 \left(\frac{\text{pCi } ^{222}\text{Rn}}{\text{m}^2\text{-sec}} \Big/ \frac{\text{pCi } ^{226}\text{Ra}}{\text{g tailing}} \right) \times 10^{-12} \frac{Ci}{pCi}$$

$$\times 5.0 \times 10^5 \text{ m}^2 \times 3.15 \times 10^7 \frac{sec}{yr} = 7 \times 10^3 \frac{Ci}{yr} . \quad (12.8)$$

Particulates

The release of radioactive particulates by wind erosion of tailings is a function of wind speed, area, concentration, and the distribution of

94

radioactive concentrations. The emission rate is estimated using the equations described in Section 5.

The particulate release rates were calculated based on the following parameters:

Surface roughness height, $z_0 = 1$ cm

Density of tailings grains, $\alpha = 2.4$ g/cm^3

Average grain diameter, $d = 300$ μm

Percent of tailings mass that is smaller than 20 μm, $p = 3.0$

Specific activity of radionuclide i in tailings with particle size less

than 20 μm in diameter, I_{20}:

^{238}U	$450 \times 0.07 \times 2.4 = 75.6$ pCi/g
^{234}U	$450 \times 0.07 \times 2.4 = 75.6$ pCi/g
^{230}Th	$450 \times 0.95 \times 2.4 = 1026$ pCi/g
^{226}Ra	$450 \times 0.998 \times 2.4 = 1078$ pCi/g
^{210}Pb	$450 \times 0.998 \times 2.4 = 1078$ pCi/g
^{210}Po	$450 \times 0.998 \times 2.4 = 1078$ pCi/g

The activity fraction of suspended particulate for sizes less than 20 μm in diameter was assumed to be $F_{20} = 0.4$. Moisture in surface tailings was assumed to be the average $W = 0.1\%$.

The sample problem input data together with the Job Control Cards required to run the program on IBM 370/195 are listed in Appendix B. The printed output and the concentration plots from the sample problem are provided in Appendix C.